

NOTICE CONCERNING COPYRIGHT RESTRICTIONS

This document may contain copyrighted materials. These materials have been made available for use in research, teaching, and private study, but may not be used for any commercial purpose. Users may not otherwise copy, reproduce, retransmit, distribute, publish, commercially exploit or otherwise transfer any material.

The copyright law of the United States (Title 17, United States Code) governs the making of photocopies or other reproductions of copyrighted material.

Under certain conditions specified in the law, libraries and archives are authorized to furnish a photocopy or other reproduction. One of these specific conditions is that the photocopy or reproduction is not to be "used for any purpose other than private study, scholarship, or research." If a user makes a request for, or later uses, a photocopy or reproduction for purposes in excess of "fair use," that user may be liable for copyright infringement.

This institution reserves the right to refuse to accept a copying order if, in its judgment, fulfillment of the order would involve violation of copyright law.

T.G.I.

01200

UF
RHS
GPHY
TL
001

DOE/ET/28392-26

19328

19328

ELECTRIC FIELD RATIO TELLURIC SURVEY OF THE ROOSEVELT HOT SPRINGS, UTAH

by

Karen Carlston

Work performed under Contract No.

DE-AC07-78ET28392

Department of Geology and Geophysics

University of Utah

Salt Lake City, Utah (USA)

March, 1982

Prepared for
DEPARTMENT OF ENERGY
Division of Geothermal Energy

Trans-Pacific Geothermal, inc.
LIBRARY

ELECTRIC FIELD RATIO TELLURIC SURVEY OF THE
ROOSEVELT HOT SPRINGS, UTAH

by

Karen Carlston

March, 1982

Department of Geology & Geophysics
University of Utah
Salt Lake City, Utah

NOTICE

This report was prepared to document work sponsored by the United States Government. Neither the United States nor its agent, the United States Department of Energy, nor any Federal employees, nor any of their contractors, subcontractors or their employees, makes any warranty, express or implied, or assumes any legal liability or responsibility for the accuracy, completeness, or usefulness of any information, apparatus, product or process disclosed, or represents that its use would not infringe privately owned rights.

NOTICE

Reference to a company or product name does not imply approval or recommendation of the product by the University of Utah or the U.S. Department of Energy to the exclusion of others that may be suitable.

TABLE OF CONTENTS

	Page
ABSTRACT	1
INTRODUCTION	3
GEOLOGIC SETTING	5
FIELD INSTRUMENTS	7
FIELD MEASUREMENTS	8
QUALITATIVE INTERPRETATION	13
QUANTITATIVE INTERPRETATION	19
Line 2200	25
Line 4000	29
Line 5950	30
CONCLUSIONS	33
ACKNOWLEDGEMENTS	34
REFERENCES	35
LIST OF FIGURES	38

ABSTRACT

In beginning exploration in the vicinity of a suspected geothermal system, a rapid reconnaissance electrical survey is important to locate regions worthy of more detailed study. The electric field ratio telluric method is a reconnaissance technique which employs a collinear three-electrode array to measure the successive electric field ratios along a profile. To afford some depth discrimination, frequencies of .05 Hz and 8 Hz, both showing large amplitudes on a natural field spectrum, are commonly measured.

An electric field ratio telluric survey during the summer of 1979 over the Roosevelt Hot Springs Known Geothermal Resource Area (KGRA) failed to consistently delineate regions of lower resistivity surrounding the major N-S faults which localize hot spring activity.

While each of the four profiles, measured perpendicular to the local strike, show a signature over previously mapped major faults, the magnitudes of response and the shapes of the curves vary in such a way that it is difficult to locate faults definitively or even to separate major faults from surficial lateral conductivity contrasts. Any such contrast which reaches the surface causes significant edge effects due to discontinuity of the horizontal perpendicular electric field; averaging these anomalous values over a dipole length can bias the shapes of the curves such that deeper structures are not detectable.

Previous and more quantitative electrical surveys over the Roosevelt Hot Springs yielded resistivity cross sections from which relative electric field curves have been calculated and then compared with telluric ratio field data. CSAMT data (Sandberg and Hohmann, 1980) at 34, 98, 977, and 5208 Hz led to resistivity models which compare poorly with telluric ratio field data. The comparison of field data curves with profiles calculated from dipole-dipole resistivity models suggests the necessity of a bedrock layer at a depth shallower than 600 meters, the depth extent of the model. Models derived from EM sounding data in conjunction with Schlumberger sounding data show a good fit to field data.

INTRODUCTION

Lightning discharges and current flow in the ionosphere give rise to natural electromagnetic fields which can be used for exploring the upper several kilometers of the earth's crust. The electric field ratio telluric method is a qualitative, reconnaissance method applicable to large survey areas where rapid and relatively inexpensive profiles are desired. The telluric survey conducted during the summer of 1979 is one of several electrical method studies done by the University of Utah over the Roosevelt Hot Springs since 1974.

Conducting a reconnaissance survey over a region in which more detailed studies have already been done yields data which can be correlated with previous results, thus the telluric ratio technique could be tested as a preliminary exploration tool for similar geothermal systems.

This technique essentially concerns the measurement of conductivity. Increased conductivity in a hydrothermal environment can be explained by two mechanisms: electrolytic conduction which is greater near hot springs because of higher effective porosities and temperatures, and surface conduction which is increased in the presence of clays due to a thin zone of cations which are attracted to the net negative charge of the clay mineral surfaces. The lowered resistivities result in smaller electric fields which can be measured and used to outline a geothermal system. Active hot springs in the Basin and Range

Province are characterized by steeply dipping, N-S normal faults which localize hot spring activity. Clay alteration products often parallel these faults and may persist to several hundred meters depth (Beyer, 1977).

Previous work (Beyer, 1977) by Lawrence Berkeley Laboratory near Leach Hot Springs, Nevada, showed the electric field ratio telluric method to be a useful technique for the initial stages of geothermal exploration. The method successfully delineated low-resistivity regions, with good repeatability, and the telluric data correlated well with dipole-dipole and bipole-dipole resistivity results.

GEOLOGIC SETTING

Previous geologic studies of the Mineral Mountains include those of Condie (1960), Petersen (1975), Evans (1977), Yusas and Bruhn (1979), and Nielson and others, (1978).

The geology of the Roosevelt Hot Springs region is dominated by repeated volcanism and intrusions. The area is composed of one large (32 km by 8 km) granitic pluton, approximately 35 m.y. old, flanked by Cretaceous and Paleozoic sedimentary units and Precambrian metamorphics to the West. Quaternary rhyolitic volcanics (.5 to .8 m.y.) are exposed in the central part of the range. Although the thermal source of the Roosevelt Hot Springs has not been determined, it has been hypothesized (Nielson and others, 1978) that this most recent volcanism may indicate the presence of an upper level magma chamber which could serve as a heat source to the geothermal system. If such a chamber remains molten or partially melted today, it may be electrically conductive and, therefore, detectable by telluric or magnetotelluric electrical surveys.

The Roosevelt Hot Springs KGRA is controlled by the following four fault systems: 1) large-scale low-angle faults formed during the Tertiary uplift of the Mineral Mountains, 2) northwest-trending fault zones which are related to the low-angle faults, 3) east-west steeply dipping faults which are thought to have formed the east-west valleys along the western margin of the range, and 4) the youngest faults in the area, the north- to northeast-trending normal faults which localize hot

spring activity, the Opal Dome Fault being one such structure. Figure 1 is a map of previously determined fractures in the KGRA.

Of central interest to electrical surveys is the hydrothermally altered rock in the vicinity of the Roosevelt Hot Springs. Feldspars have been altered by acid-sulfate water and replaced by clay, muscovite, opal and chalcedony (Parry and others, 1978). Alteration reaches a maximum depth of 2 km with clay minerals transitioning to a stable K-feldspar regime between 200 and 400 meters depth near the Opal Dome Fault. The granitic rocks of the Mineral Mountain pluton are weathered to greater than 500 feet.

Subsurface information and identification of drill cuttings are described thoroughly by Nielson and others, (1978). The drill hole data show that Quaternary alluvium is underlain by Precambrian bedrock to the west of the Opal Dome Fault, while bedrock to the east of the fault is granitic.

FIELD INSTRUMENTS

Telluric field data were collected using a receiver designed and constructed at the Lawrence Berkeley Laboratory (Beyer, 1977). The LBL Mark III A Telluric Receiver includes high- and low-pass filters tunable to .01 Hz and 1000 Hz, respectively, amplifiers with gains of 10 to 2000, and integration circuitry for handling the 8 Hz signals.

The outputs of the two-channel receiver were applied to the X and Y inputs of an X-Y plotter. Two plotters were used: a Hewlett Packard 7035A X-Y Recorder, and a Series 2000 Omnigraphic X-Y Recorder. The Omnigraphic recorder has sensitivity ranging from .2 mv/cm to 10 v/cm, while the sensitivity of the Hewlett Packard ranges from .4 mv/cm to 4 v/cm. Neither device is advisable for field use because circuitry and mechanical parts are not sufficiently shielded--dust posed a real problem, requiring regular cleaning of gliding arms and cables.

Non-polarizing copper-copper sulfate porous pot electrodes were used.

FIELD MEASUREMENTS

Using the electric field ratio telluric method, it is possible to obtain a relative amplitude profile of the component of the electric field in the direction of the measured traverse. To accomplish this, three electrodes are emplaced with the center electrode common, forming two collinear dipoles across which the time-varying electric field is measured. The averaged instantaneous electric field from each dipole is then amplified and filtered by the LBL receiver and used as the X and Y inputs of an X-Y recorder.

It is important that the incident telluric field be a plane wave over the dimensions of the survey area. Previous studies (Srivastava, 1965) and good repeatability of data for other telluric surveys (Beyer, 1977) has shown this assumption to be valid. The incident field for telluric surveys can be assumed to be a downward propagating plane wave having a time harmonic variation of $e^{i\omega t}$. The averaged electric fields across the two dipoles are then

$$E_1 = E_1^0 e^{(i\omega t + \theta_1)}$$
$$E_2 = E_2^0 e^{(i\omega t + \theta_2)}$$

where

E^0 = wave amplitude

$\theta_2 - \theta_1 = \theta$ = phase difference between the two dipoles.

The fields, E_1 and E_2 , are input to the X and Y terminals of an X-Y recorder. The plotter draws an ellipse with dimensions described by the parameters $2E_1^\circ$ and $2E_2^\circ$, the constant maximum electric field amplitudes, or by the useful measurements of tilt angle, ϕ , and ellipticity, ϵ . Figure 2 illustrates these parameters. The ellipse has a negative slope because of the reversed polarity of one dipole.

Although the phase of the earth's telluric field measured perpendicular to the strike of a two-dimensional inhomogeneity is small, it is not necessarily zero. Tilt angle becomes progressively worse, as an approximation of E_2°/E_1° , as ellipticity increases, and as tilt angle deviates from $\pm 45^\circ$. Beyer (1977) has shown that for tilt angles ranging from 15° to 75° with ellipticities less than .1, the error in measuring tilt angle instead of E_2°/E_1° , is less than 7%. The tilt angles measured in the field ranged from 15° to 70° and, with the exceptions of data collected for Line N-S, all ellipticities were less than .07. Measuring tilt angle therefore imposed negligible errors for determining the relative electric fields between two dipoles.

To obtain a continuous set of relative electric field intensity ratios, the array was leapfrogged along the survey line. A relative amplitude profile was then obtained by successively multiplying the station measurements together. Figure 3 shows the dipole configuration and illustrates the method for obtaining a relative amplitude profile.

To afford some depth discrimination, two frequencies were measured, .05 Hz (bandpass filter setting of .03 Hz and .05 Hz), and 8 Hz (filter setting of 6 Hz and 10 Hz). Both frequencies show large amplitudes on a power spectrum of the earth's electromagnetic field. The

characteristics of the natural electromagnetic field, as applied to geophysical exploration techniques, have been studied by others (Wait, 1954; Ward, 1967) and will not be dealt with here.

Because no X-Y plotter can accommodate a frequency of 8 Hz, the oscillations being too rapid for the mechanical workings of the recorder, the signal is rectified and stored capacitively. The resulting voltages are then used as the inputs to the X and Y terminals of the X-Y recorder. The signal traces a line of positive slope. A slow capacitor discharge rate then allows the pen to reseek its origin. The slope of the line made by the burst is equivalent to the time-averaged electric field ratio measured over the two dipoles (Beyer, 1977).

The .05 Hz data require no such circuitry manipulation. Signals are filtered, amplified and put directly into the X and Y inputs of the plotter, and the ellipse is traced. Figures 4 and 5 show representative data obtained at .05 Hz and 8 Hz, respectively. The repeated 45° slopes are calibration lines measured to insure that signals from each dipole are amplified equally.

Figure 6 shows the location of the four profiles measured over the Roosevelt KGRA. Line 2200, Line 4000 and Line 5950 are perpendicular or nearly perpendicular to the dominant north-south local strike.

Wannamaker and others (1980) have shown that, over the Roosevelt Hot Springs, resistivity contrasts can be considered to be two-dimensional for TM-mode magnetotelluric data, which simplifies the interpretation in that it validates the application of two-dimensional modeling techniques.

The north-south line was unusual in that good data could not be obtained even after repeated trials over several days. It is possible that one or several three-dimensional features near station 900 of this line introduce a large phase difference between the two dipoles, observed on the plotter as large ellipticity. Figure 7 shows the best data obtained for station 1500 of Line N-S. At stations 1800 and 2100 the readings were much worse. Because only three stations could be measured over Line N-S at each frequency, no attempt is made to interpret data over this line.

Line 2200 traverses the Opal Dome Fault where surface opal, chalcedony and siliceous sinter deposits are abundant. Thirteen stations were measured at a dipole spacing of 300 meters.

Dipoles for Line 4000 are also spaced at 300 meters. Station 1500 of this line is approximately 100 meters directly north of drill hole DDH1A, which provided useful information for estimating depths to resistivity interfaces. Eleven stations were recorded. Seven stations were measured at 600 meter dipole spacing over Line 5950.

Ellipticities measured in the field were generally small, less than 0.07, and tilt angles measured over several periods show little variation, thus the data were repeatable. Near the end of the field season several stations of each line were reoccupied; the results were good, the largest deviation from the averaged previous reading being 3°.

Obtaining good data was a problem when the telluric signal was low due to low sunspot activity, verified by listening to WWV radio broadcasts, or when the 8-Hz signal from thunderstorms was very low, usually a problem during the morning hours. When such conditions were

observed, good 8 Hz readings could be obtained by waiting for the occasional burst of signal. Low (.05-Hz) signals often persisted for several days. Under such conditions the best data possible were recorded.

Some erratic readings were caused by wind, observed as aperiodic bursts of signal on one dipole only, or seen on the receiver as independent sweeps of the needles of the voltmeters. It became practice to pile dirt on top of the dipole wires to keep the wires flat on the ground. Except on the most windy days, the effects of the wind were thereby avoidable.

On several occasions, due to receiver or plotter malfunction, the calibration line would not trace over itself.

QUALITATIVE INTERPRETATION

Any information derived from telluric ratio data is qualitative in nature. It is not possible to determine an absolute relation between the electric field ratios and apparent resistivities as in more quantitative methods such as magnetotelluric or dipole-dipole resistivity studies. Measuring only two frequencies severely limits depth discrimination, but measuring over a larger range of frequencies would negate the advantages of this technique - its low cost and rapidity of data acquisition. It is not practical, then, to attempt to derive resistivity versus depth cross sections from telluric ratio data alone, because any resistivity model which provides a good fit would be highly nonunique; a large number of models could show an equally good fit. Instead, the electric field ratio profiles, drill hole data, and the geologic map of the Roosevelt Hot Springs (Nielson and others, 1978) have been used to verify known faults and fractures, to outline alteration zones and to distinguish near-surface contrasts from deeper structures.

Figures 8, 9, and 10 show the relative electric field profiles calculated from the field data at 8 Hz and .05 Hz for Line 2200, Line 4000, and Line 5950, respectively. The location of the Opal Dome Fault is shown on each figure.

All three lines show an increase from west to east in the electric field and, therefore, a proportional increase in apparent resistivity.

Because all profiles are perpendicular to the major fault zone, the strike component of the magnetic field in the presence of a two-dimensional inhomogeneity is invariant with distance from the fault, and a ratio of the electric fields over the two dipoles is proportional to the ratio of the two resistivities. In fact, if the telluric intensity were measured simultaneously on either side of a lateral two-dimensional conductivity contrast, and distant from it, the ratio of the electric field measured over the two dipoles would be equal to the square root of the ratio of corresponding apparent resistivities. Unfortunately, the Roosevelt Hot Springs area is characterized by multiple lateral conductivity inhomogeneities; the curves do not reach asymptotic values, and relative apparent resistivity ratios cannot be calculated.

Lines 2200, 4000, and 5950 all show signatures over the Opal Dome Fault. Each signature is different, however, and it would be difficult, upon observation of each profile, to map the Opal Dome and other faults without prior knowledge of their locations.

The Opal Dome Fault at Line 2200 appears to have a significant lateral conductivity contrast which reaches the surface. This would be necessary for the sharp "overshoot" and "undershoot" to appear in the curves. Beyer (1977) has shown that a thin homogeneous layer at the surface will diminish or eliminate such edge effects, which are due to the discontinuity in the horizontal electric field at the surface.

Relative electric field curves for Line 2200 are similar for both frequencies in the vicinity of and to the west of the Opal Dome Fault; no lateral contrasts occur at a depth which the .05 Hz signal reaches

but the 8 Hz does not. To the east, the 8 Hz data increase more rapidly than the .05 Hz data, reaching an amplitude sixteen times greater than the field measured at the west end of the profile. The .05 Hz field increases to nearly six times that of the west end. For both frequencies, the abrupt increase in the relative electric field marks the general edge of the sedimentary basin and the proximity to the exposed tertiary intrusives. It is possible that the large 8 Hz anomaly is due to highly resistive material near the surface which is underlain by material of lower resistivity which the 8 Hz signal does not reach.

It is important to remember that the skin depth for such low frequencies is quite large and the depth of burial must be significant with respect to the skin depth in order to observe such a difference between the 8 Hz and the .05 Hz curve. Below are shown skin depths for both frequencies for representative resistivities.

<u>Resistivity (ohm-meters)</u>	<u>Skin depth at 8 Hz (meters)</u>	<u>Skin depth at .05 Hz (meters)</u>
1	180	2250
5	400	5020
10	560	7110
50	1260	15890
100	1780	22500
500	3970	50240

Profile 4000 shows a general low of the electric field amplitude in the region of the fault. No "overshoot" or "undershoot" is observed, an indication that surface conductivity changes are more gradual than those observed near Line 2200.

Lowered resistivity over a geothermal system can be due to (a) fractures in the rock causing an increase in the effective porosity, thereby increasing the mobility of ions in a saline solution, or (b) clay alteration which causes an increase in conductivity by surface conduction. Ward and Sill (1976) have shown that clay in core samples from the altered zone will reduce resistivities by a factor of 2 to 4.

Drill hole DDH1A, which is located near station 1500 of Line 4000, has the following alteration products (Parry and others, 1978):

<u>Depth</u>	<u>Alteration Product</u>
6m - 18m	Alunite
18m - 16m	Alunite, kaolinite
26m - 32m	Alunite ± kaolinite
WATER TABLE 35m	
32m - 56m	montmorillonite, kaolinite, k-mica
56m - 66m	montmorillonite, kaolinite, + 2% pyrite

Lowered resistivity due to clay alteration has been estimated to be insignificant at 400 meters (Ward and Sill, 1976; Parry and others, 1978).

The presence of montmorillonite, which has a high ion exchange capacity (Ward and Sill, 1976), and pyrite, as well as the presence of water below the water table, should increase the mineral surface conductivity below 35 meters to a depth no greater than 400 meters.

It is likely that brine has leaked or is leaking from the convective hydrothermal system. The result of such leakage would be a resistive surface layer underlain by brine-saturated alluvium. In fact, first-separation, 1-km, dipole-dipole pseudosections have shown

resistivities as low as 1 Ωm to occur at depths of 100 meters to 300 meters well to the west of the Opal Dome Fault (Ward and Sill, 1976).

The relative electric fields over Line 4000 show little difference between the 8 Hz and .05 Hz curves, especially west of the fault. The possibility of lowered resistivity resulting from brine leakage is not shown by the electric field ratio telluric data. Any such interface occurs at a depth which is too shallow to cause any difference between the 8-Hz and .05-Hz responses.

The plot of the 8 Hz field on Line 4000 is almost identical to that of the .05-Hz relative field, indicating that there is no large lateral conductivity contrast below the depth of exploration of the 8 Hz signal.

The electric field curves for Line 5950 are similar in shape for both frequencies, showing a gradual increase in the field from west to east. The .05-Hz profile shows a more rapid increase, however, than does the 8 Hz profile, which is the opposite of the responses observed over Line 2200 and Line 4000.

The dipole lengths used for Line 5950 were twice the length used for the other lines; any small-scale perturbations in the electric field due to near-surface contrasts would tend to be averaged out. Line 5950 is farther from recent hot spring activity and traverses fewer mapped faults than does Line 4000. In the absence of such near-surface two-dimensional structures the field changes would naturally be more gradual. In fact, a first-separation dipole-dipole resistivity contour map at 300 meter dipole spacings does show gentle character north of Negro Mag Wash.

There is a sharp increase in the electric field near the location of the Opal Dome Fault. It is difficult to tell from these curves alone which side of the fault is upthrown. Because the field is averaged over 600 meters, any "undershoot" or "overshoot" which might give a sense of direction is smoothed out. Also, the anomaly over the fault is only a single dipole anomaly. An interpretation of the sense of motion or an attempt to locate faults is not possible from this profile alone. Although 500 meters is the common electrode spacing used for telluric ratio surveys, shorter dipole lengths give more information about surface features; 300 meter spacings, or even shorter intervals near faults, should therefore be maintained over a geothermal system with large surface variations.

The differences in amplitude between the two frequencies indicate that deeper structures are distinguishable, to some extent, from shallow ones. At some depth beyond the penetration of the 8-Hz signal the resistivity increases more rapidly from west to east than does the resistivity near the surface.

QUANTITATIVE INTERPRETATION

Calculated relative electric field curves resulting from models derived from dipole-dipole resistivity studies (Ross, and others, 1981), controlled-source audiomagnetotelluric (CSAMT) data (Sandberg and Hohmann, 1980), and Schlumberger resistivity and electromagnetic data (Tripp, 1977) are compared with telluric ratio field data below.

The computer program used for calculating theoretical curves was developed by Stodt (1978). It employs the finite element approach for solution of geophysical problems governed by the two-dimensional inhomogeneous scalar Helmholtz equation. In this case, the electromagnetic responses of two-dimensional resistivity models were calculated for an incident field of the transverse magnetic (TM) mode. Because all profiles measured were perpendicular to the local strike, only the perpendicular electric field component was necessary to calculate relative electric field profiles.

Nutter (1979) wrote an interactive version of this program that also was used.

To obtain a relative amplitude profile from the computer output, averages of the electric field over intervals of 300 meters for Line 2200 and Line 4000, and over intervals of 600 meters for Line 5950 were calculated, these representing the dipole lengths used in the field. It was necessary to compute a weighted average because the program calculates the electric field at points on a grid, the nodes

being more closely spaced near conductivity contrasts. The averages were weighted by multiplying the electric field by the horizontal distance over which the field is calculated. The averaged electric field over a dipole was then calculated as:

$$E = \frac{\sum_{i=1}^N E_i \Delta \ell_i}{\sum_{i=1}^N \Delta \ell_i}$$

where $\Delta \ell_i$ = interval length between nodes

E_i = value of electric field at a node

N = number of nodes

Electric field ratios were then successively multiplied to obtain an electric field profile relative to the averaged field measured over the westernmost dipole.

Beyer (1977) used a similar program and produced a catalog of curves for various two-dimensional models. He also studied the effects of varying 1) the traverse line direction with respect to strike, 2) the incident electromagnetic field ellipticity, and 3) the polarization direction. His curves were used when possible to estimate the magnitudes of response and shapes of the curves expected over various bodies.

For computation of the electromagnetic field, models are not truncated at the edges or bottom as suggested by the model diagrams; they extend in these respective directions for several skin depths such that the secondary fields, due to conductivity contrasts located near

the center of the model, have become negligible at the boundaries of the computational field. Because the only necessary calculations involve the TM mode, it is not required to extend the air layer in a similar manner as would have been done if the TE mode had been used.

Telluric ratio data for Line 2200 are compared with profiles calculated from models obtained using the CSAMT method (Sandberg and Hohmann, 1980) and the dipole-dipole resistivity method (Ross and others, 1981). Field curves of Line 4000 are compared with calculated results for models derived from dipole-dipole resistivity data (Ross and others, 1981), Schlumberger resistivity data taken along Line 3500N (Tripp, 1977), and for a model derived from CSAMT data (Sandberg and Hohmann, 1980). Line 5950 is compared with curves derived from Schlumberger resistivity models (Tripp, 1977) and dipole-dipole resistivity models (Ross and others, 1981).

The models derived using the active-source methods explore shallower depths than what might be detectable using natural source methods at these low frequencies. In resistive ground, the electric field ratio telluric method could potentially explore depths of 20 kilometers or more. Over a geothermal region resistivities could be as low as several ohm-meters, but the skin depth at .05 Hz, which is 2000 meters at 1 Ω m and 7000 m at 10 Ω m, is still much greater than represented by the active-source models. The models derived using active-source methods show low resistivities, as low as 5 ohm-meters, which persist to the bottoms of the models or 600 meters depth. It is unlikely that such low resistivities continue to the greater depths explored by the telluric ratio method, especially east of the Opal Dome

Fault, where unaltered bedrock is estimated to begin at a depth of less than 500 meters.

As described above, the finite element program requires that the model extend to several skin depths below the deepest conductivity change. It seemed likely that such shallow models would not provide a valid means of comparison with telluric ratio data. To test the effect of vertical conductivity contrasts below the deepest lateral change, a 300 ohm-meter layer representing bedrock was added to dipole-dipole resistivity models at 600 meters for Line 2200 and Line 5950 and at 450 meters for Line 4000. Figures 11 and 12 compare the fields resulting from the original models and the modified models for Lines 4000 and 5950. Relative profiles for Line 2200 showed similar results. It appears that the electric field ratio for any model will not be greatly affected by the addition of any layered resistivity contrast beneath the deepest previously modeled structure.

Because the resistivity cross sections are modeled to a maximum depth of 600 meters and because the electrical field ratio telluric method could potentially explore much greater depths, it is important to consider the effect on the relative electric field plots of a 2-D inhomogeneity at depths greater than 600 meters. A lateral conductivity contrast at such depths could be due to faults or possibly to lowered resistivities of a partial melt.

Beyer (1977) has shown that a vertical resistive body of large depth extent will yield a larger anomaly than a horizontal resistive body of large lateral extent; the vertical body poses a larger obstruction to horizontal current flow. The Opal Dome Fault in the

dipole-dipole model for Line 2200 (Figure 14) is represented as a vertical contact between resistive (100 ohm-meters) material to the east of station 1500 and conductive (20 ohm-meters) material to the west. To be compatible with the finite element solution, the contact extends several skin depths below the deepest horizontal resistivity contrast. The .05 Hz signal sees, because of its large skin depth, a resistive block of vertical dimensions extending much deeper than 600 meters, and a large anomaly at .05 Hz might be expected. Modifying the model by adding the horizontal bedrock layer at 600 meters effectively truncates the vertical block but does not significantly change the relative field plot. This indicates that the telluric ratio method, when used in a complex geoelectrical environment, is not sensitive to lateral conductivity changes at depth greater than the depths represented by the models.

Although the skin depth at .05 Hz is large, the depth of exploration might be much shallower and may not permit detection of lowered resistivities accompanying a partial melt. Wannamaker and others (1980) conclude that the near-surface contrasts mask the deeper structures.

The ability of the electric field ratio telluric method to detect a possible melt near the Roosevelt Hot Springs depends upon the depth and size of the associated low-resistivity zone, its conductivity, and the surrounding resistivities.

The upper boundary of the thermal source has been estimated to be between 2 km (Wannamaker and others, 1980) and 5 km (Ward and Sill, 1976) with resistivities of a 700°C rhyolitic melt between 5 Ω m and 100

Ωm (Wannamaker and others, 1980). The largest resistivities for surrounding bedrock expected in the Basin and Range Province at depths between 2 and 5 km is 500 Ωm (Brace, 1971). The probable resistivity contrasts between the country rock and a partial melt could then lie between 100:1 and 3:1. The estimated largest anomaly would therefore be a large conductive block at 100:1 contrast buried 2 km.

Beyer (1977) modeled a massive conductive body of 2-km vertical dimension and 4-km horizontal dimension at a depth of 2 km within a homogeneous half-space. The conductivity contrast was 100:1. Relative electric field profiles calculated from this model are a reasonable estimate of the largest possible anomaly arising from a partial melt beneath the Roosevelt Hot Springs. The minimum relative electric field amplitude resulting from this model is .45 relative to a background level of 1. This is a small anomaly in comparison with anomalies arising from surface features, and it is likely that shallow features would indeed mask deeper ones. Also the anomalous amplitudes due to a body at depth near the Roosevelt Hot Springs could be greatly reduced by the overlying conductivity layer resulting from brine-saturated alluvium or could be shielded by a resistive steam zone (Ward and Sill, 1976; Wannamaker and others, 1980).

Beyer showed that conductive bodies with large lateral extent yield much larger anomalies, because of coupling with telluric current, than those which are of large vertical extent. Determining the lower boundary of a conductive zone is, therefore, not as important as the lateral extent.

No estimates of the horizontal extent of a potential thermal source have been made, but the surface expression would cover large horizontal distances, larger than the distances covered by the telluric ratio profiles. The .05 Hz calculated relative electric field plots could show a portion of the response due to a partial melt but it would be difficult to quantify, and shallow model comparisons, while useful for interpreting near-surface structures, will not aid much in the delineation of a thermal source. Any interpretation regarding the location of a partial melt using telluric ratio data alone is speculative at best.

Figure 13 shows a representative plot of the electric field values as output from the finite element program before averages were taken over the dipole lengths and ratios were made. Comparing the plots with the model cross section clearly points out the bias imposed on deeper structures because of surface contrasts. The sharp increases or decreases in the curves which coincide with surface conductivity changes would substantially raise or lower the weighted averages taken over dipoles containing such lateral contrasts. The effect due to the surface discontinuity is about the same at each frequency.

Line 2200

Figure 14 shows the dipole-dipole resistivity model for Line 2200 designed by Ross and others (1981). Figures 15 and 16 show a comparison between electric field ratio profiles calculated from this model and the field data profiles for .05 Hz and 8 Hz, respectively. The original model was obtained by correlating resistivity pseudosections, resistivity contour maps, geologic maps and drill hole

data, after which adjustments were made to the model until calculated resistivity pseudosections sufficiently matched the observed resistivity pseudosections (Ross and others, 1981).

The theoretical electric field ratio plots show a reasonable fit to field data near the western end of Line 2200. The field data profile shows only small variations in the relative electric field, an indication of no large-magnitude surface contrasts.

The 100 Ω m block east of station 1500 is detected by the .05-Hz signal causing a general increase from west to east in the relative electric field plot. Due to attenuation, the 8-Hz field does not show such an increase.

A lateral contrast of large magnitude which reaches the surface, the 100 ohm-meter block east of station 3000, does show a large anomaly for both .05 Hz and 8 Hz, the fields increasing by four times between stations 2700 and 3000 for both frequencies. This modeled block compares well with .05 Hz field data but fits the 8 Hz data poorly. The 8 Hz relative field computed from the model does not increase nearly as rapidly as the 8 Hz field data. The near-surface resistivities must therefore increase from west to east more rapidly than is shown by the model. Because a more extreme increase in surface resistivities would also affect the .05 Hz response, it is not possible to predict a unique resistivity structure which would better fit both the 8 Hz and .05 field data.

The "overshoot" and "undershoot" seen in the field data over the Opal Dome Fault are not seen in the curves resulting from the model, indicating that the surface resistivity contrast might be larger than

that modeled. The 100 ohm-meter block modeled near station 3000 does appear to cause edge effects, observed as a decrease in the electric field ratio as the contact is approached from the conductive side resulting from a downward component of current flow into the resistive medium.

Field data for Line 2200 are compared with theoretical curves calculated from a model derived using CSAMT data (Sandberg and Hohmann, 1980). Connecting one-dimensional MT inversion results of the CSAMT TM mode data at each station along Line 2200 yielded a two-dimensional resistivity model which was then revised by applying the aforementioned two-dimensional finite element program and adjusting the model to fit the CSAMT field data. Figure 19 shows the resulting model. Figures 17 and 18 compare the relative electric field amplitude plots calculated from this model for .05 Hz and 8 Hz, respectively, with the telluric ratio field data.

The 300 ohm-meter block modeled at 155 m depth just west of the Opal Mound Fault is detected easily by the .05 Hz data and causes a large anomaly, much larger than that observed in the field. The modeled 8 Hz anomaly is much smaller, due to attenuation.

Sandberg incorporated a gravity interpretation (Crebs, 1976) which shows a 230 m wide bedrock horst buried at 30 m representing the upthrown block to the west of the Opal Dome Fault, and interpreted slightly increased apparent resistivity measured at the lowest frequency of 32 Hz to model the bedrock block. A resistivity of 300 ohm-meters was used to coincide with the bedrock resistivity modeled for Line 4000.

The resistive structure modeled from dipole-dipole resistivity data, a 100 ohm-meter block buried at 300 m, fits the telluric ratio data better than the 300 ohm-meter block buried at 155 m modeled from CSAMT data. This is not surprising when the depths of exploration for both methods are considered. The skin depth in 10 ohm-meter material at 32 Hz is only 280 m and Sandberg found, using sensitivity tests, that the depth of exploration is less than a skin depth, while the dipole-dipole technique at $n=4$ has a depth of exploration of approximately 400 meters. The skin depth at .05 Hz for a 10 ohm-meter material is 7100 m.

Based on telluric ratio results, the 100 ohm-meter block at 300 m depth is a better representation of the deep structure near the Opal Dome Fault than the resistive block modeled from CSAMT data.

The CSAMT model contains a sharp increase in resistivity east of station 2400 which is similar to the contrast modeled by the dipole-dipole data. Neither model reflects the large observed anomaly. A better fit to field data might be obtained by modeling a larger surface contrast underlain by a block of lower resistivity. However, the block of lower resistivity must be buried deep enough that attenuation lessens the 8 Hz response to the conductive block. Such a model would yield an anomaly which is larger at 8 Hz than at .05 Hz. The skin depth at 8 Hz for 10 Ωm material, the lowest resistivity at the east end of the profile, is 360 meters and the skin depth for 200 Ωm material, the highest modeled resistivity, is 12,550 meters. A conductive block buried below 12,550 meters would lower the .05 Hz response while not changing the 8 Hz amplitude. The effect on the 8 Hz curve would probably be minimal at depths much greater than 360 meters.

The depth extent of the model is only 270 meters.

Line 4000

The models derived for Line 4000 from Schlumberger and electromagnetic sounding data (Tripp, 1977), CSAMT data (Sandberg and Hohmann, 1980) and dipole-dipole resistivity data (Ross and others, 1981) are shown in Figures 20, 25, and 26, respectively. Calculated relative electric field curves from these models are compared with 8 Hz and .05 Hz field data below.

The Schlumberger-EM model was designed using one-dimensional inversion results of both EM data and Schlumberger data. The resistivity of the basement was constrained to 300 ohm-meters. Due to the lack of Schlumberger soundings east of station 2400, the model was designed to be compatible with a previous dipole-dipole model (Ward and Sill, 1976).

The relative electric field curves calculated using the EM-Schlumberger resistivity model correlate better with telluric ratio field data than either the curves derived from CSAMT model or the dipole-dipole resistivity model. The relative electric field profile calculated using the CSAMT data does not compare well with the field data. Because the CSAMT study used higher frequencies than those measured in the telluric ratio survey, a good comparison may not be a reasonable expectation.

All three cross sections model a conductive unit with resistive overburden to the west end of the profile. The conductive material, which represents lowered resistivity resulting from brine leakage away from the convective hydrothermal system, is not distinguishable by electric field ratio telluric methods. The 8 Hz and .05 Hz field data

were nearly identical west of the Opal Dome Fault, again showing the minimal role of skin effect attenuation at such shallow depths.

The theoretical curves derived from Schlumberger resistivity soundings show excellent comparison with telluric ratio profiles (Figures 21 and 22), the only significant deviation from field data being at the east end of the line for 8 Hz. The 8-Hz field curve shows a larger increase to the east than does the calculated curve. By bringing the 300 ohm-meter block modeled east of the fault nearer to the surface, a better fit would be made with the electric field ratio telluric data.

The CSAMT model compares fairly well over the fault and to the west of the fault for both frequencies, but provides a bad fit to the east (Figures 23 and 24). Sandberg states that resolution at lower frequencies was poor and, although he does show a 200 ohm-meter block at the easternmost end of his model, the telluric ratio data suggest that a resistive structure is needed west of the 200 ohm-meter block.

The dipole-dipole resistivity cross section does not model bedrock, represented as 300 Ω m material. The poor fit for both frequencies at both the west and east ends of the profile (Figures 27 and 28) can be explained by the absence of resistive material. The fact that the Schlumberger resistivity models provide such a good fit to telluric profiles for both frequencies indicates that a resistive structure at depth is needed.

Line 5950

Relative electric field profiles calculated from field data are compared with theoretical profiles derived from a dipole-dipole model,

(Ross and others, 1981) shown in Figure 31, and a Schlumberger-EM sounding model shown in Figure 32.

The calculation relative electric field from the dipole-dipole model compares poorly with field results as seen in Figures 29 and 30. The large relative magnitude shown in the theoretical profiles at station 2400 is not present in the field data curves. The anomalous magnitude at station 2400 and the increase in the electric field east of station 3600 are shown at both frequencies but are more pronounced at .05 Hz. Except for the 100 ohm-meter material toward the eastern end of the profile and the 150 ohm-meter shallow block between stations 000 and 2400, the modeled resistivities are low, the largest portion of the geoelectric section having resistivities below 20 ohm-meters. The skin depth for 20 ohm-meter material at .05 Hz is 10.1 km, and at 8 Hz it is 0.79 km. Theoretical anomalies are probably smaller at 8 Hz because of attenuation of the 8 Hz field. The general trend of the calculated curves is quite different from the observed relative fields, theoretical curves increasing as the observed curves decrease and vice versa.

A dipole length of 500 meters is a common electrode spacing used in the field (Beyer, 1977). To achieve greater resolution, 300 meter spacings were used for Line 2200 and Line 4000. To cover more ground in less time, 600 meter spacings were used for Line 5950. Longer dipole lengths will average out many of the edge effects due to minor lateral surface discontinuities. For this reason and for greater efficiency, 500 or 600 meter dipole lengths are adequate if deep large-magnitude structures are the exploration target. If information about the surface character of a geothermal system is desired, a spacing of 250 to 300 meters is necessary.

A comparison between field data curves for Line 5950 and curves resulting from Schlumberger and EM data will be discussed very briefly. Figures 33 and 34 show the theoretical and observed profiles resulting from the model shown in Figure 32. The entire model designed by Tripp is contained within three dipole lengths of the telluric ratio profile. Tripp's survey of Line 5950 was more detailed, covering one-third the horizontal distance covered by the telluric survey. The relative field profiles calculated from the Schlumberger model fit the field data slightly better than the curves resulting from the dipole-dipole model. The general trend is the same, but the relative field magnitudes near the Opal Dome Fault are larger for the theoretical curves than those observed in the field.

CONCLUSIONS

If the electric field ratio telluric method is used as a reconnaissance tool, interpretations based on this method alone should be qualitative only. Depth discrimination is very limited down to the lowest frequency due to the bias imposed by surface conductivity contrasts. It is doubtful that a thermal source at a depth of 2 km or greater could be detected in a geothermal system usually characterized by a complex geoelectric section containing large lateral surface conductivity contrasts.

The technique does give the general expression of the near-surface conductivity changes over the Roosevelt Hot Springs. Line 4000 shows a broad but distinctive resistivity low near the Opal Dome Fault, which would be adequate evidence to recommend more extensive studies. Line 2200 shows a signature over the same fault, seen as an "overshoot" and "undershoot" on the relative electric field profile, but the data would be difficult to interpret without prior knowledge of the surrounding structures. Profiles over Line 5950 increase from west to east, possibly tracing a rough image of the sedimentary basin.

The electric field telluric ratio method should be restricted to large survey areas where large anomalies are expected, and where there are no major non-surface lateral resistivity changes due to features other than geothermal manifestations. The Basin and Range Province is not such a place.

ACKNOWLEDGMENTS

Funding for this project came from the Department of Energy, Division of Geothermal Energy contract number DOE-AC07-78ET2892.

I would like to thank many people for their help and support during this project, including Gerald Hohmann, William Sill, William Nash, William Frangos, and Carleen Nutter.

References

- Beyer, H., Dey, A., Liaw, A., Majer, E., McEvelly, T. V., Morrison, H. F., and Wollenberg, H., 1976, Preliminary open file report, geological and geophysical studies in Grass Valley, Nevada: Lawrence Berkeley Lab., report LBL-5262, 144 p.
- Beyer, J. H., 1977, Telluric and D. C. resistivity techniques applied to the geophysical investigation of Basin and Range geothermal systems, Part I: the E-field ratio telluric method: Lawrence Berkeley Lab., report LBL-6325 1/3, 135 p.
- Brace, W. F., 1971, Resistivity of Saturated Crustal Rocks to 40 km Based on Laboratory Measurements, *in* The Structure and Physical Properties of the Earth's Crust: AGU Monograph 14, p. 243-256.
- Cagniard, L., 1953, Basic theory of the magneto-telluric method of geophysical prospecting: Geophysics, v. 18, no. 3, p. 605-635.
- Condie, K. C., 1960, Petrogenesis of the Mineral Range Pluton, Southwestern Utah: Univ. Utah, M.S. Thesis, 92 p.
- Crebs, T. J., 1976, Regional gravity survey of the central Mineral Mountains including detailed gravity and ground magnetic surveys of the Roosevelt Hot Springs area: Univ. Utah, M.S. Thesis, 129 p.
- Evans, S. H., 1977, Geologic map of the central and northern Mineral Mountains, Utah: Technical report v. 77-7, DOE/DGE contract EY-76-S-07-1601: Univ. Utah, Dept. Geol. Geophys.
- Neuenschwander, E. F., and Metcalf, D. F., 1942, A study of electrical earth noise: Geophysics, v. VII, no. 1, p. 69-77.
- Nielson, D. L., Sibbett, B. S., McKinney, D. B., Hulen, J. B., Moore, J. N., Samberg, S. M., 1978, Geology of Roosevelt Hot Springs KGRA, Beaver County, Utah: Univ. Utah Res. Inst., Earth Science Lab., report ESL-12, 120 p.
- Nutter, C., 1979, An interactive modeling system for 2-D, magneto-telluric and line source resistivity data (MT2D users guide and documentation): Univ. Utah, Geol. Geophys. Dept., report DOE/ID/12079-1, 178 p.

- Parry, W. T., Bryant, N. L., Dedolph, R. E., Ballantyne, J. M., Ballantyne, G. H., Rores, D. T., and Mason, J. L., 1978, Hydrothermal Alteration at the Roosevelt Hot Springs Thermal Area, Utah: Univ. Utah, Geol. Geophys. Dept., report DOE/ET/28392-17, 29 p.
- Petersen, C. A., 1975, Geology of the Roosevelt Hot Springs area, Beaver County, Utah: Utah Geology, v. 2, no. 2, p. 109-116.
- Ross, H. P., Nielson, D. L., Smith, C., Glenn, W. E., Moore, J. N., (1981), An integrated case study of the Roosevelt Hot Springs geothermal system, Utah: AAPG Bulletin, in press.
- Sandberg, S. K., and Hohmann, G. W., 1980, Controlled source audio-magnetotellurics in geothermal exploration: Univ. Utah, Geol. Geophys. Dept., report DOE/ID/12079-5, 85 p.
- Sill, W. R., and Johng, D. S., 1979, Self potential survey, Roosevelt Hot Springs, Utah: Univ. Utah, Geol. Geophys. Dept., report DOE/ET/28392-21, 29 p.
- Slankis, J. A., Teleford, W. M., and Becker, A., 1972, 8 Hz telluric and magnetotelluric prospecting: Geophysics, v. 37, no. 5, p. 862-878.
- Srivastava, S. P., 1965, Method of interpretation of magnetotelluric data when field source is considered: J. Geophys. Res., v. 70, p. 945-954.
- Stodt, J. A., 1978, Documentation of a finite element program for solution of geophysical problems governed by the inhomogeneous 2-D scalar Helmholtz equation: Univ. Utah, Geol. Geophys. Dept., NSF Contract No. AER 76-11155, 75 p.
- Tripp, A. C., 1977, Electromagnetic and Schlumberger resistivity sounding in the Roosevelt Hot Springs Known Geothermal Resource Area: Univ. Utah, M.S. Thesis.
- Wait, J. R., 1954, On the relation between telluric currents and the earth's magnetic field: Geophysics, v. 19, no. 2, p. 281-289.
- Wannamaker, P. E., Ward, S. H., Hohmann, G. W., and Sill, W. R., 1980, Magnetotelluric models of the Roosevelt Hot Springs thermal area, Utah: Univ. Utah, Geol. Geophys. Dept., report DOE/ET/27002-8, 213 p.

- Ward, S. H., 1967, Electromagnetic theory for geophysical application, in Mining Geophysics, v. II: Soc. Explor. Geophys., p. 10-196.
- Ward, S. H. and Sill, W. R., 1976, Dipole-dipole resistivity delineation of the near-surface zone at the Roosevelt Hot Springs area: Univ. Utah, Geol. Geophys. Dept., topical report 76-1, 9 p.
- Wescott, E. M., and Hessler, V. P., 1962, The effect of topography and geology on telluric currents: J. Geophys. Res., v. 67, no. 12, p. 4813-4823.
- Yungul, S. H., 1966, Telluric sounding -- a magnetotelluric method without magnetic measurements: Geophysics, v. 31, no. 1, p. 185-191.
- Yusas, M., and Bruhn, R., 1978, Fracture systems in the Roosevelt Hot Springs KGRA: Dept. of Geology and Geophysics, Univ. of Utah, DOE/DGE Contract EG-78-C-07-1701.
- Yusas, M. R., and Bruhn, R. L., 1979, Structural fabric and in-situ stress analyses of the Roosevelt Hot Springs KGRA: Univ. of Utah, Geol. Geophys. Dept., report DOE/ET/28392-31, 62 p.

LIST OF FIGURES

- Figure 1. Map of previously interpreted fractures showing the locations of drill holes and geothermal wells.
- Figure 2. An electric field ratio ellipse as displayed on the X-Y recorder. E_1 and E_2 are constant maximum electric field amplitudes. ψ is the tilt angle, ϵ is the ellipticity, and ϕ is the angle, whose tangent is E_2/E_1 . (The figure is taken directly from Beyer, 1977.)
- Figure 3. Illustration of the dipole configuration used in the field and a sample relative electric field profile.
- Figure 4. Representation of .05 Hz field data.
- Figure 5. Representation of 8 Hz field data.
- Figure 6. The locations of the four profiles measured over the Roosevelt Hot Springs KGRA.
- Figure 7. The best data obtained along Line N-S.
- Figure 8. The relative electric field calculated from field data over Line 2200. Both 8 Hz and .05 Hz data are shown.
- Figure 9. The relative electric field calculated from field data over Line 4000. Both 8 Hz and .05 Hz data are shown.
- Figure 10. The relative electric field calculated from field data over Line 5950. Both 8 Hz and .05 Hz data are shown.
- Figure 11. A comparison between calculated relative electric fields resulting from the model shown in Figure 26 and the relative field due to the same model with the addition of a 300 ohm-meter bedrock layer at 450 meters.

- Figure 12. A comparison between calculated relative electric fields resulting from the model shown in Figure 31 and the relative field due to the same model with the addition of a 300 ohm-meter bedrock layer at 600 meters.
- Figure 13. The electric field (not averaged) calculated from the model in Figure 14.
- Figure 14. Two-dimensional resistivity model derived from dipole-dipole sounding-profiling data along Line 2200 (from Ross et al., 1981). Resistivities are in ohm-meters. The vertical exaggeration is 4:1.
- Figure 15. A comparison between the field data profile over Line 2200 and the calculated relative electric field curves resulting from the model derived from dipole-dipole data. The frequency is .05 Hz.
- Figure 16. A comparison between the field data profile over Line 2200 and the calculated relative electric field curves resulting from the model derived from dipole-dipole data. The frequency is 8 Hz.
- Figure 17. A comparison between the field data profile over Line 2200 and the calculated relative electric field curves resulting from the model derived from CSAMT data.
- Figure 18. A comparison between the field data profile over Line 2200 and the calculated relative electric field curves resulting from the model derived from CSAMT data. The frequency is 8 Hz.
- Figure 19. Resistivity model from CSAMT data along Line 2200 (from Sandberg and Hohmann, 1980). Block resistivities are in ohm-meters. The vertical exaggeration is 5:1.
- Figure 20. Resistivity model for Schlumberger soundings along Line 3500 (from Tripp, 1977). Block resistivities are in ohm-meters. The vertical exaggeration is 4:1.

- Figure 21. A comparison between the field data profile over Line 4000 resulting from the model derived from Schlumberger resistivity data. The frequency is .05 Hz.
- Figure 22. A comparison between the field data profile over Line 4000 resulting from the model derived from Schlumberger resistivity data. The frequency is 8 Hz.
- Figure 23. A comparison between the field data profile over Line 4000 and the calculated curves resulting from the model derived from CSAMT data. The frequency is .05 Hz.
- Figure 24. A comparison between the field data profile over Line 4000 and the calculated curves resulting from the model derived from CSAMT data. The frequency is 8 Hz.
- Figure 25. Resistivity model from CSAMT data along Line 4000 (from Sandberg and Hohmann, 1980). Block resistivities are in ohm-meters. The vertical exaggeration is 5:1.
- Figure 26. Two-dimensional resistivity model derived from dipole-dipole sounding-profiling data along line 4000 (from Ross et al., 1981). Resistivities are in ohm-meters. The vertical exaggeration is 5:1.
- Figure 27. A comparison between the field data profile over Line 4000 and the calculated relative electric field curves resulting from the model derived from dipole-dipole data. The frequency is .05 Hz.
- Figure 28. A comparison between the field data profile over Line 4000 and the calculated relative electric field curves resulting from the model derived from dipole-dipole data. The frequency is 8 Hz.
- Figure 29. A comparison between the field data profile over Line 5950 and the calculated relative electric field curves resulting from the model derived from dipole-dipole data. The frequency is .05 Hz.

- Figure 30. A comparison between the field data profile over Line 5950 and the calculated relative electric field curves resulting from the model derived from dipole-dipole data. The frequency is 8 Hz.
- Figure 31. Two-dimensional resistivity model derived from dipole-dipole sounding-profiling data along Line 5950 (from Ross et al., 1981). Resistivities are in ohm-meters. The vertical exaggeration is 5:1.
- Figure 32. Resistivity model for Schlumberger soundings along Line 5950 (from Tripp, 1977). Block resistivities are in ohm-meters. The vertical exaggeration is 4:1.
- Figure 33. A comparison between the field data profile over Line 5950 and the calculated relative field curves resulting from the model derived from Schlumberger resistivity data. The frequency is .05 Hz.
- Figure 34. A comparison between the field data profile over Line 5950 and the calculated relative electric field curves resulting from the model derived using Schlumberger resistivity and EM data. The frequency is 8 Hz.

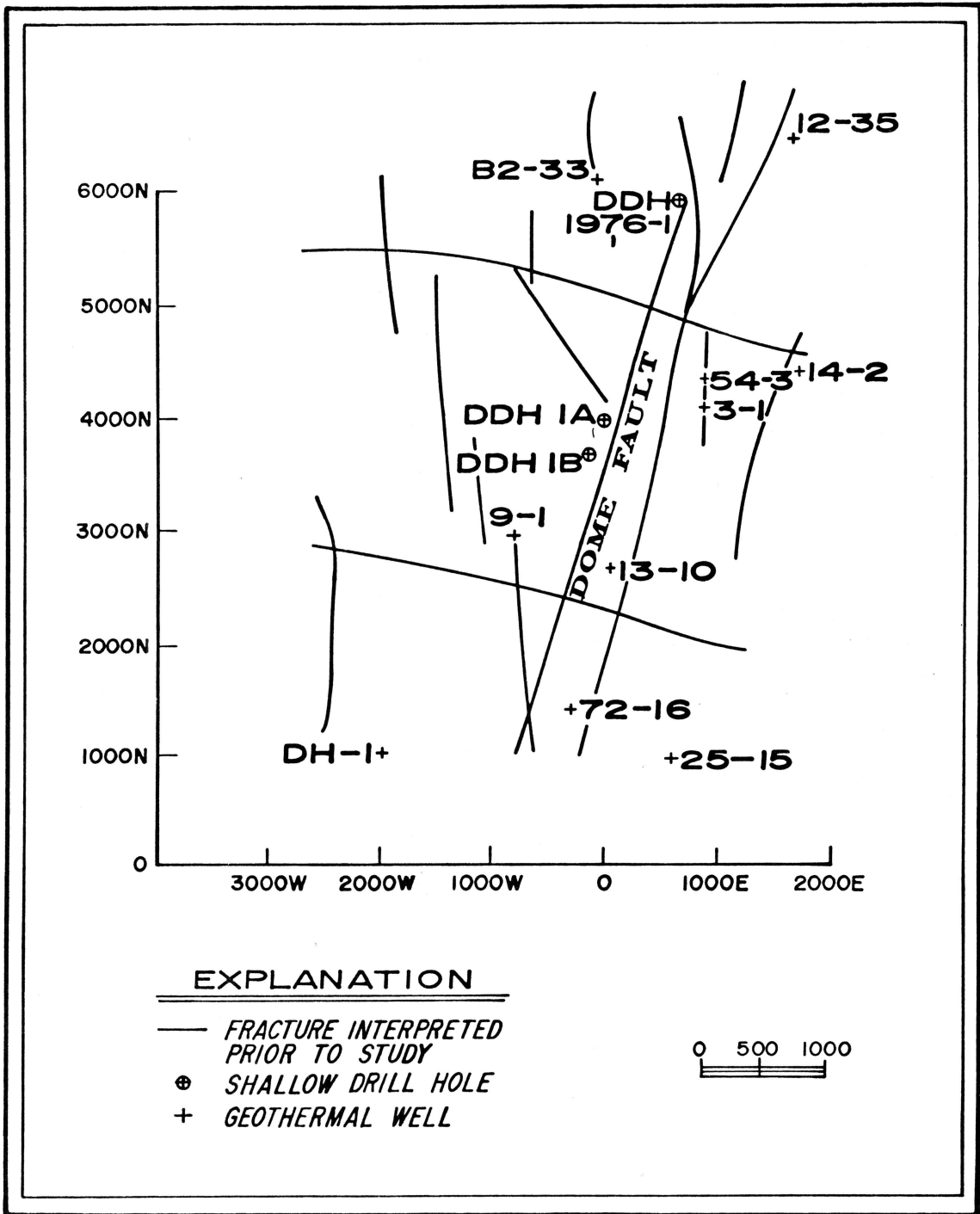


Figure 1

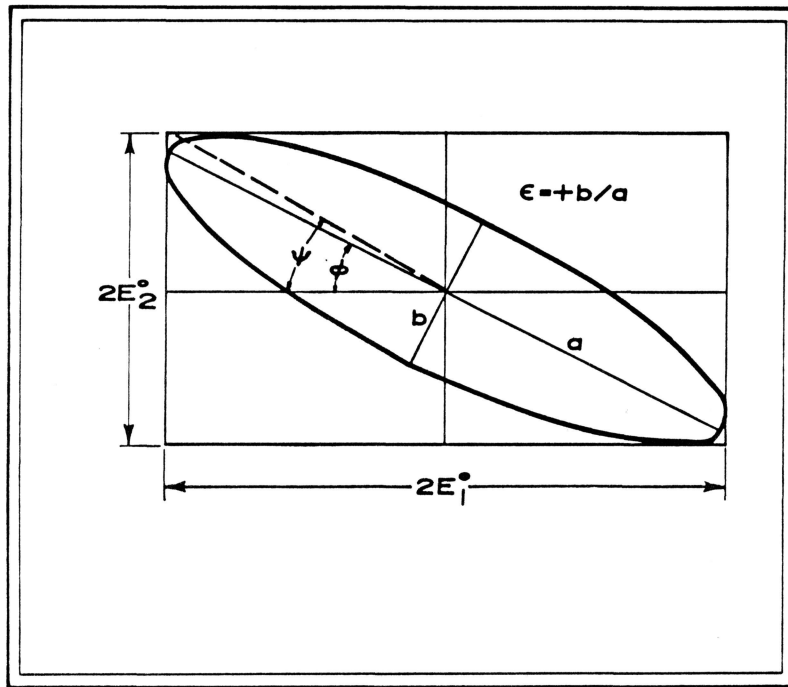


Figure 2

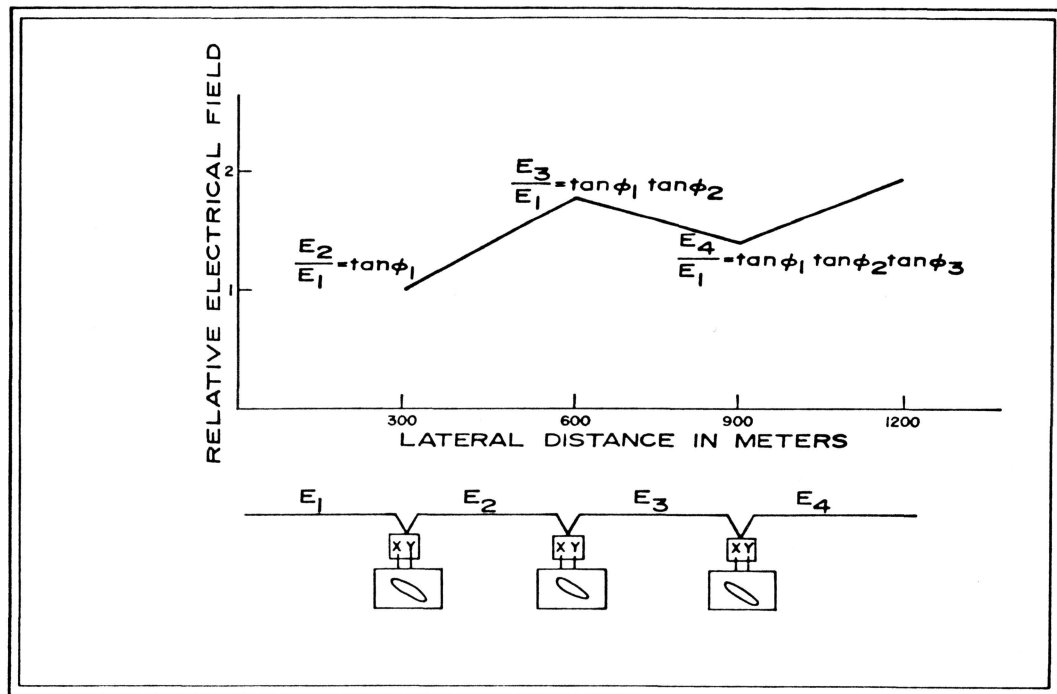


Figure 3

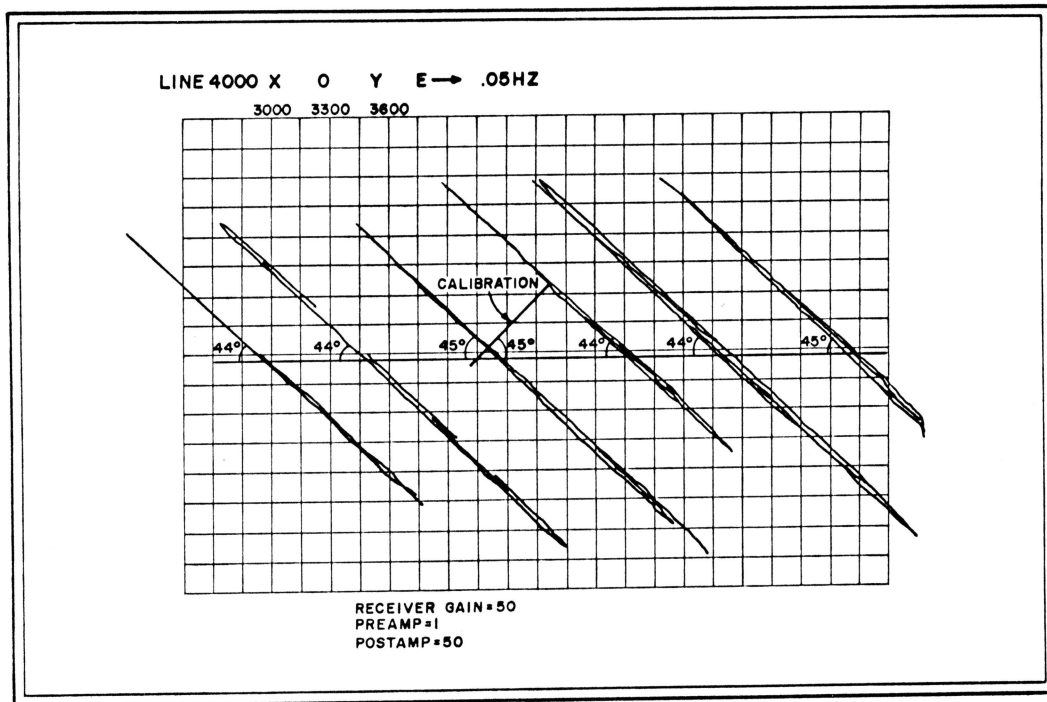


Figure 4

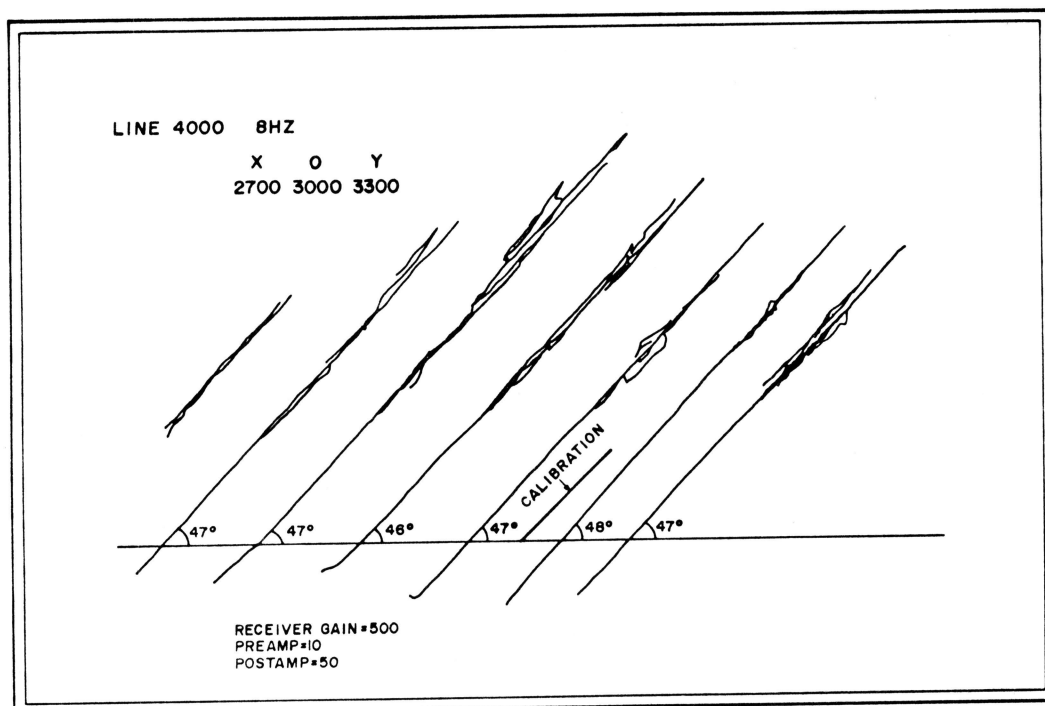
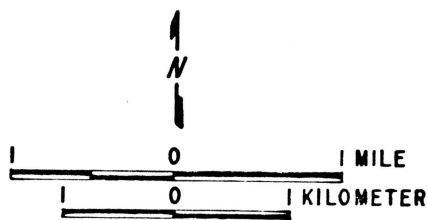
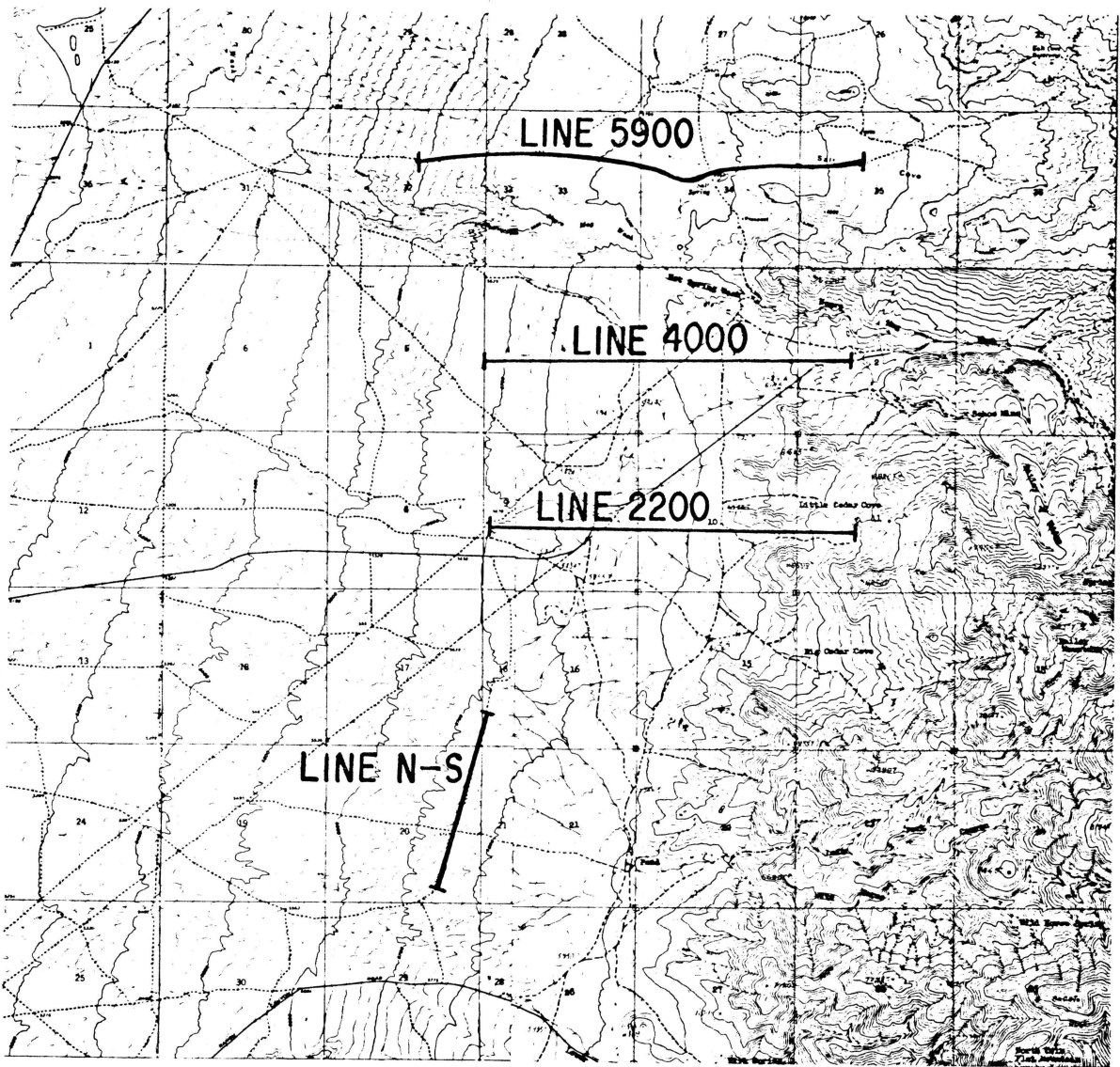


Figure 5



LINE LOCATION MAP

Figure 6

Figure 7

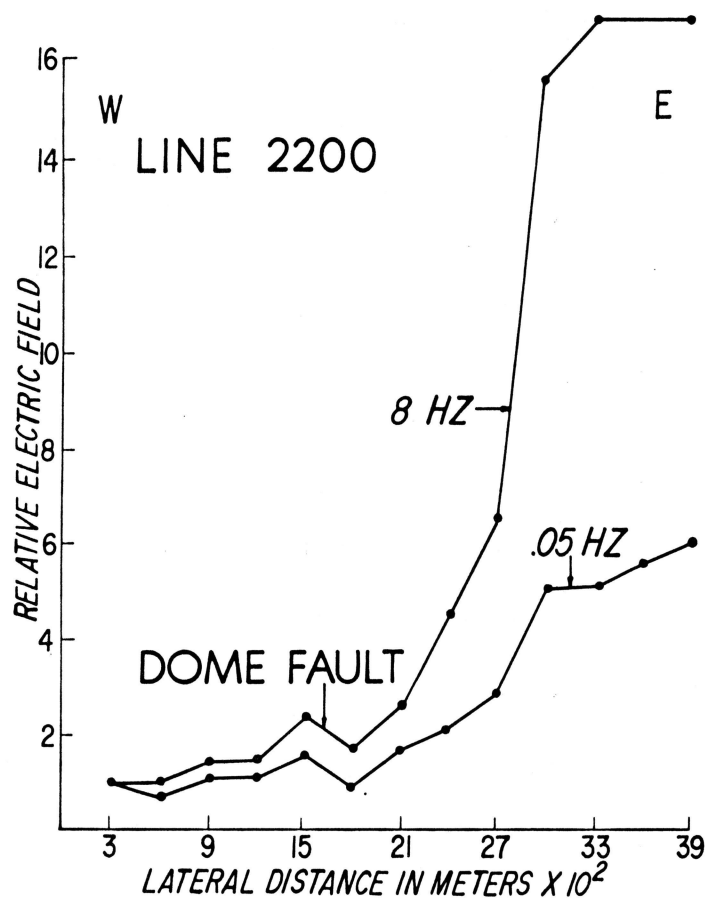
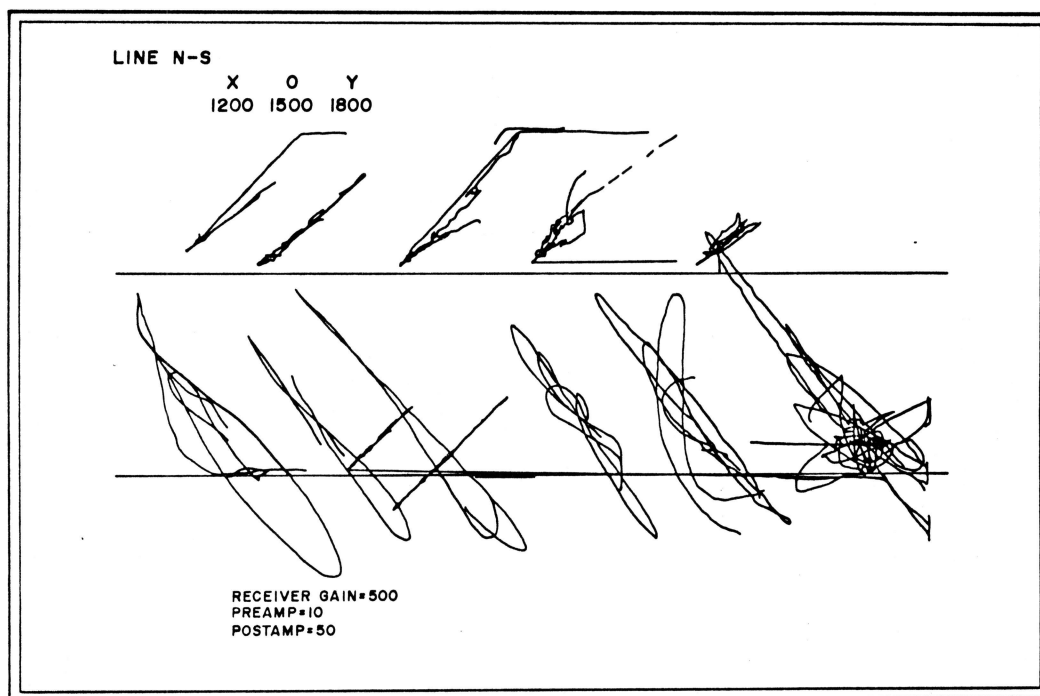


Figure 8

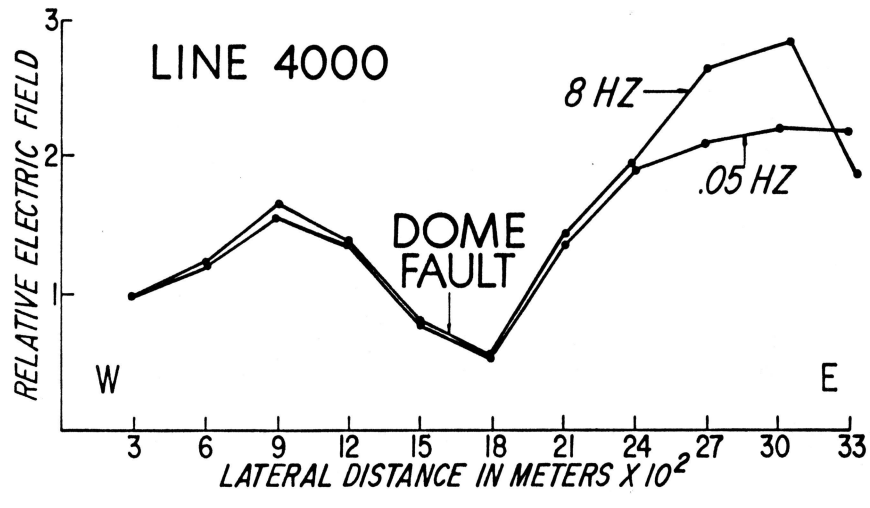


Figure 9

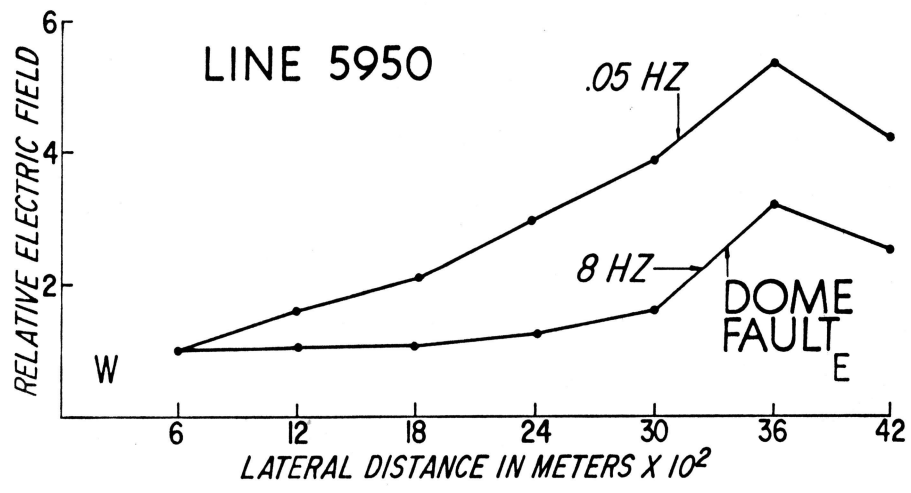


Figure 10

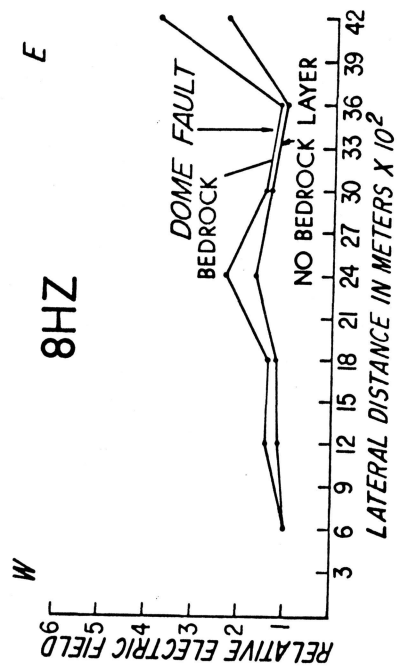
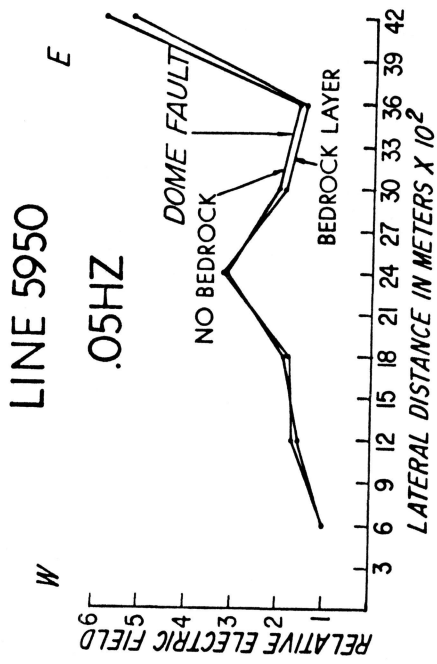


Figure 11

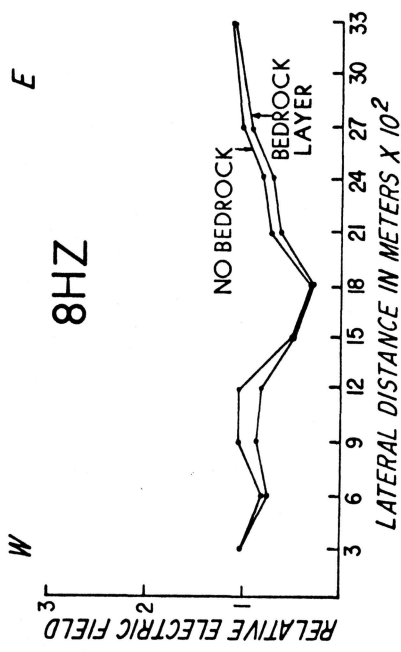
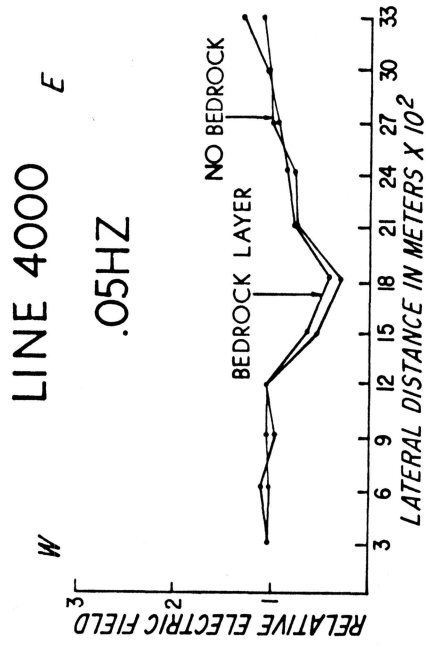


Figure 12

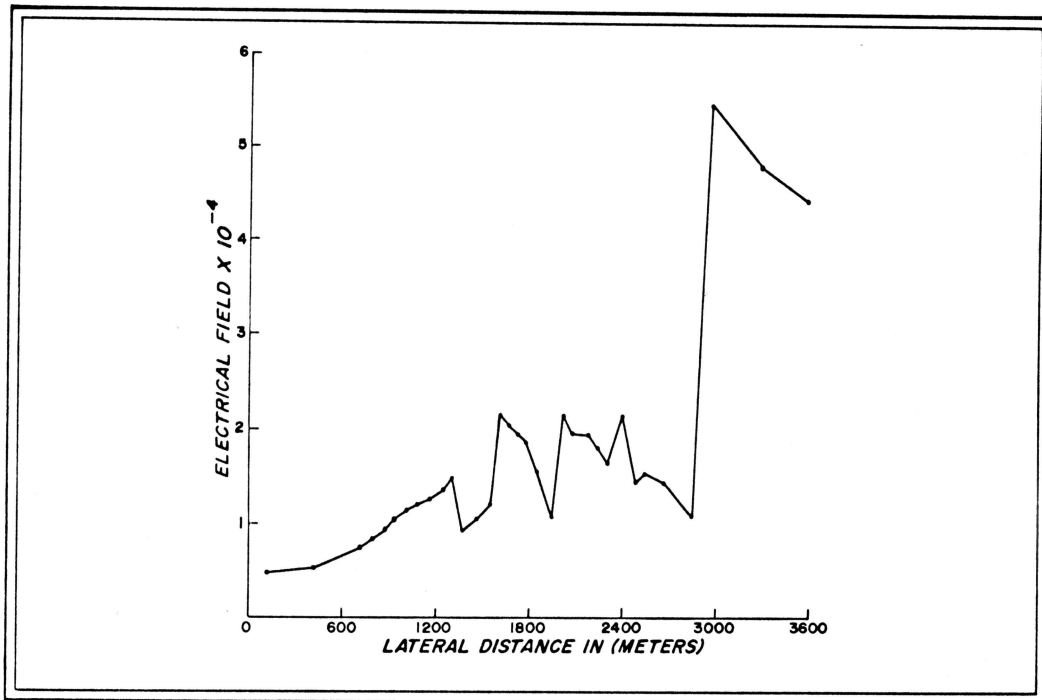


Figure 13

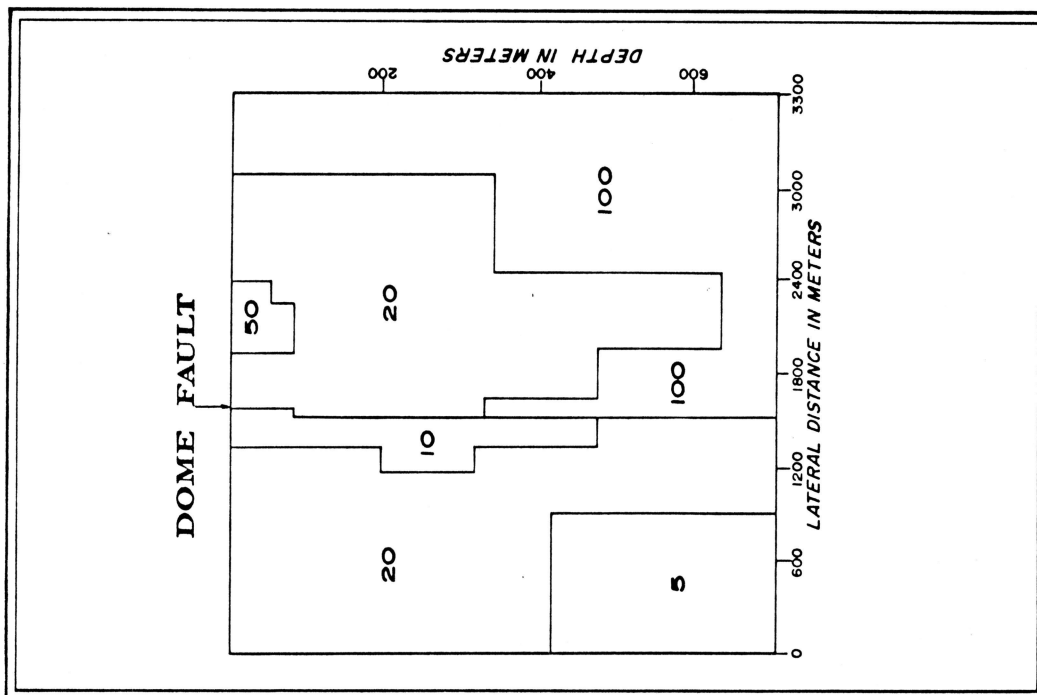


Figure 14

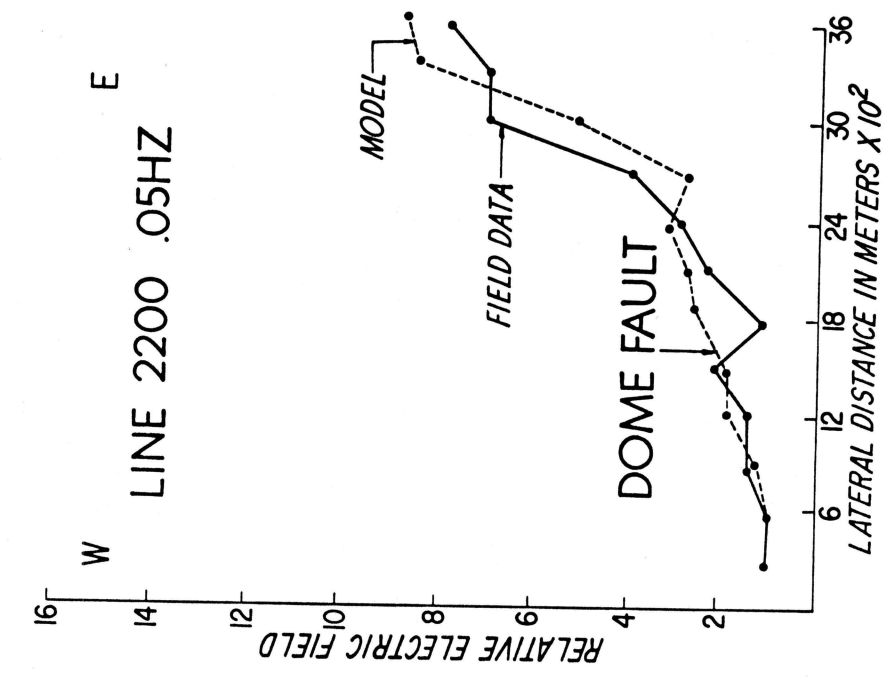


Figure 15

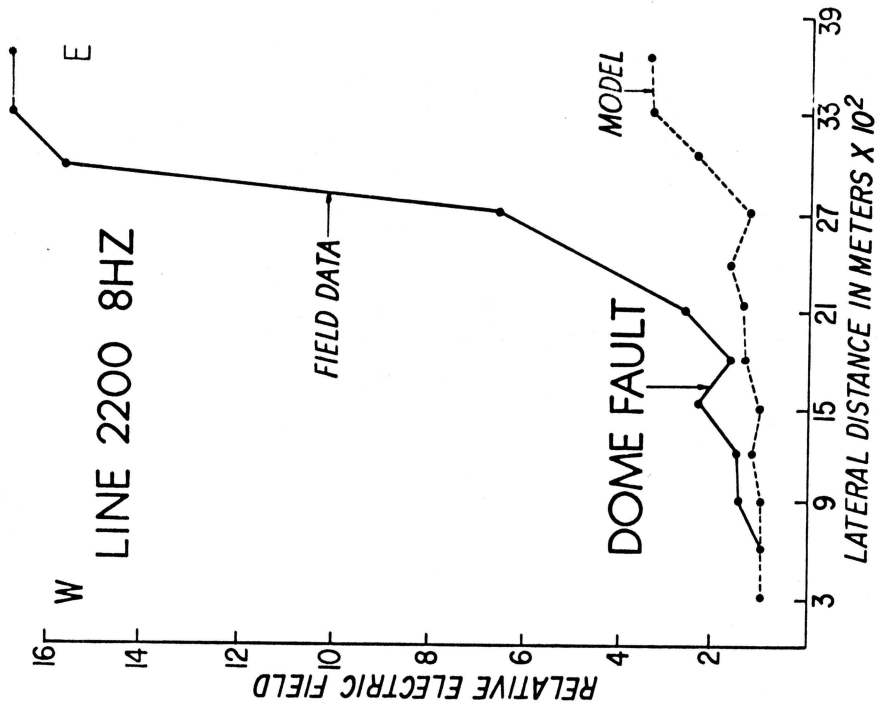


Figure 16

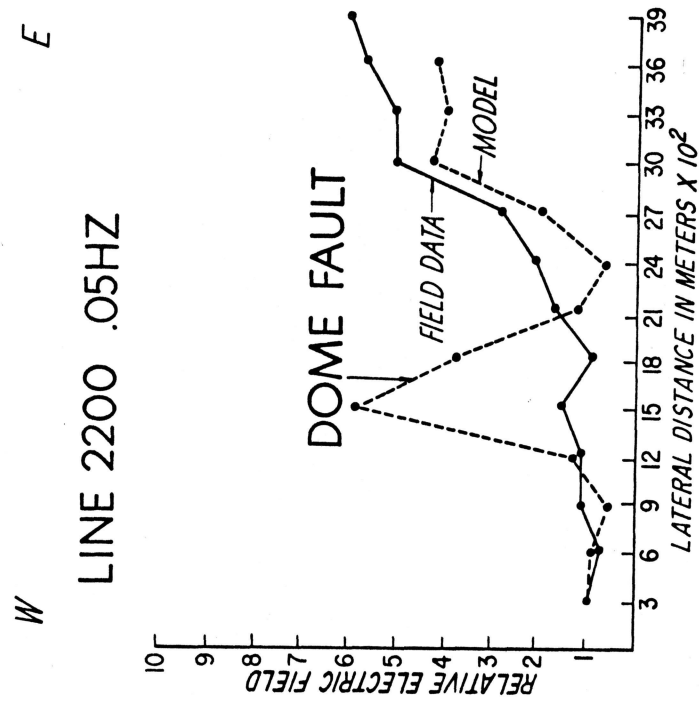


Figure 17

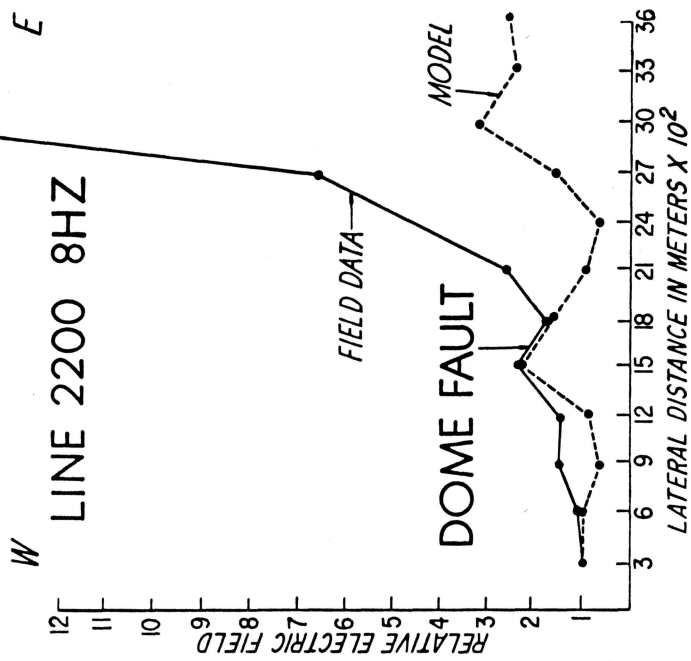


Figure 18

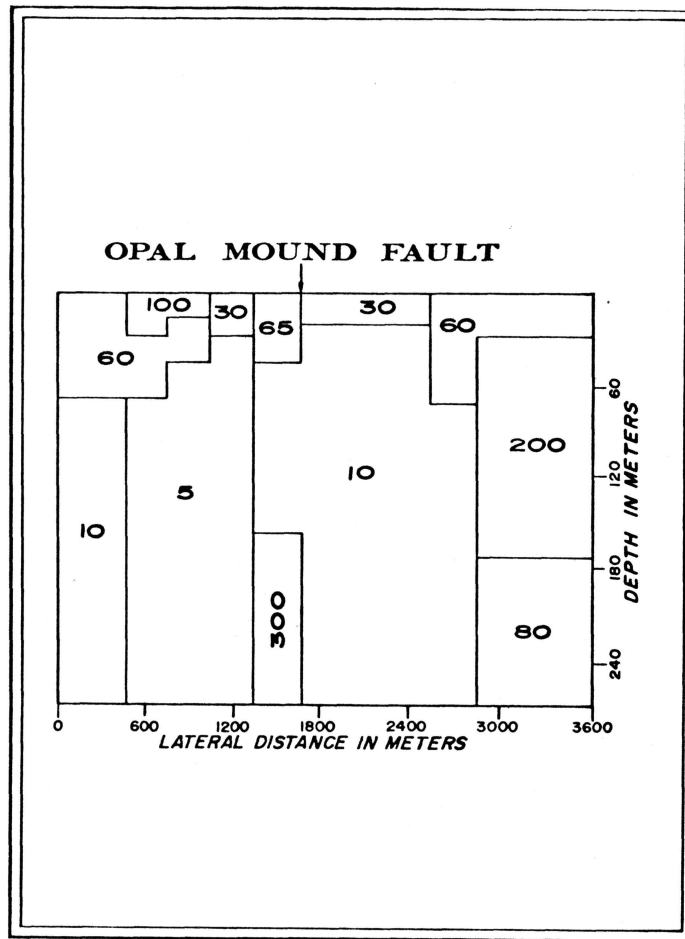


Figure 19

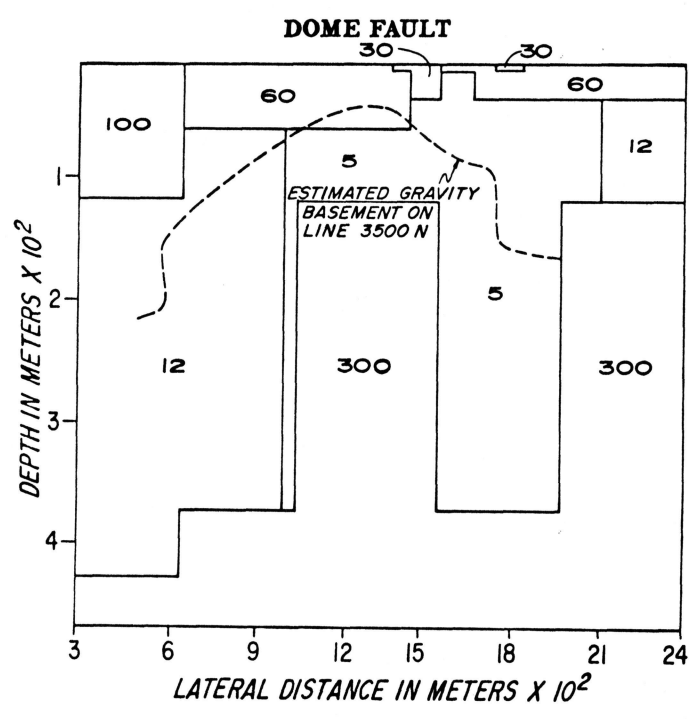


Figure 20

LINE 4000 .05HZ

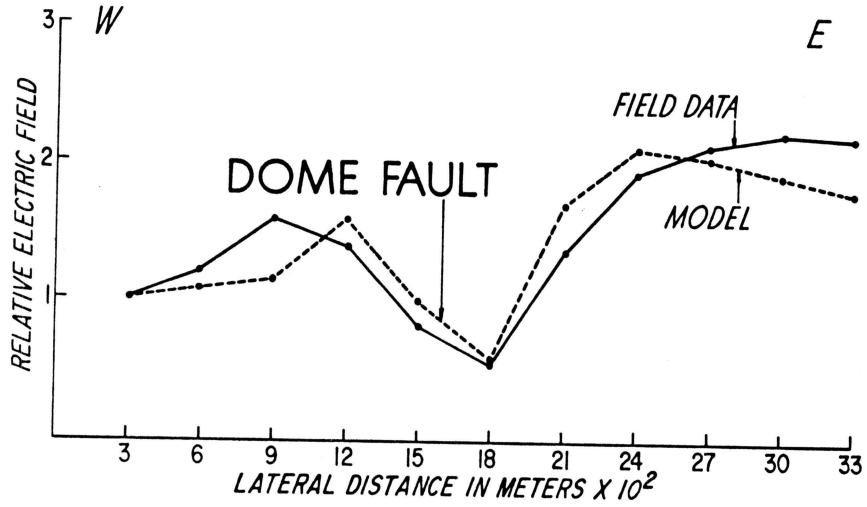


Figure 21

LINE 4000 8HZ

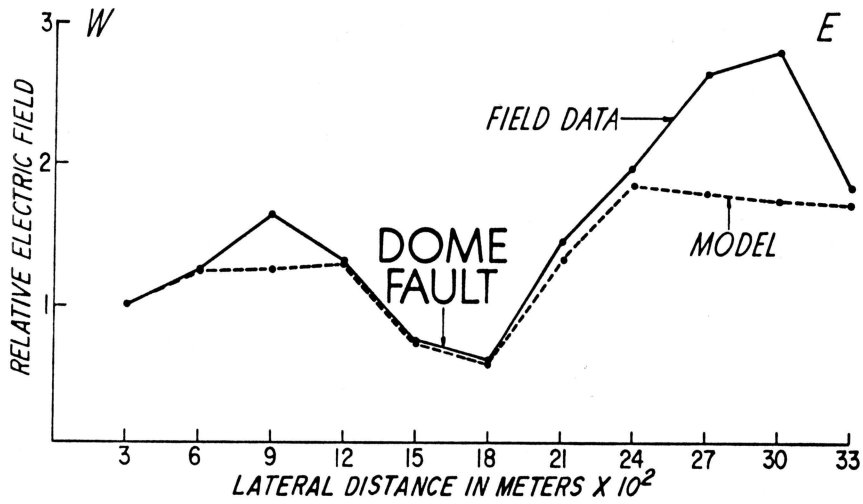


Figure 22

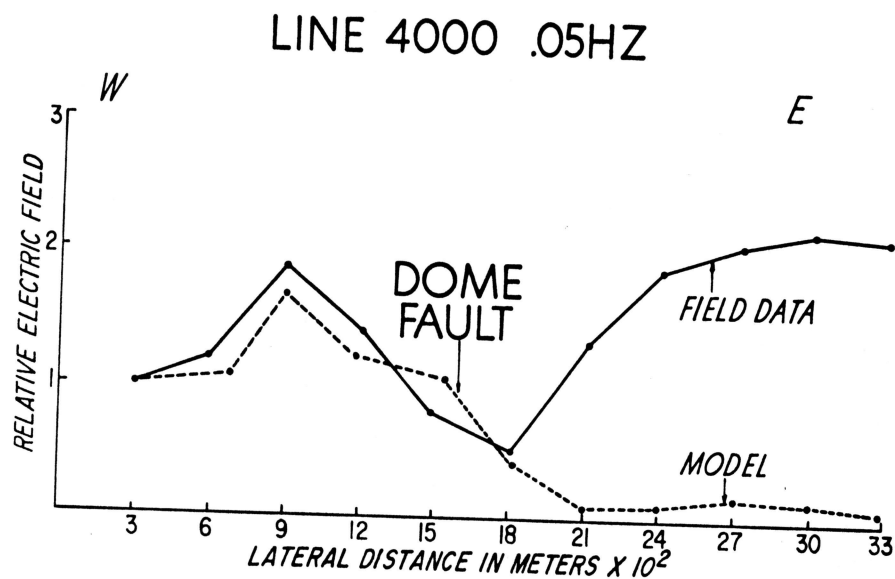


Figure 23

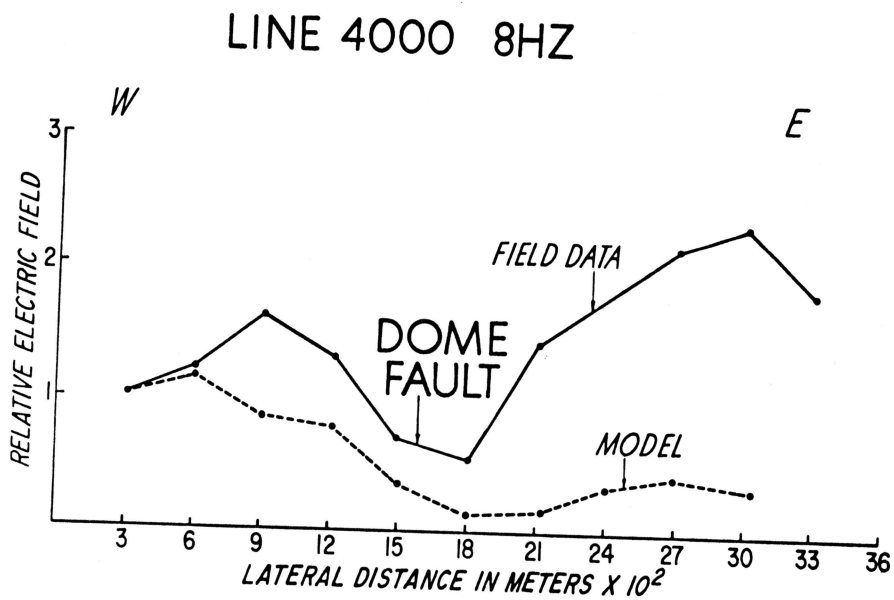


Figure 24

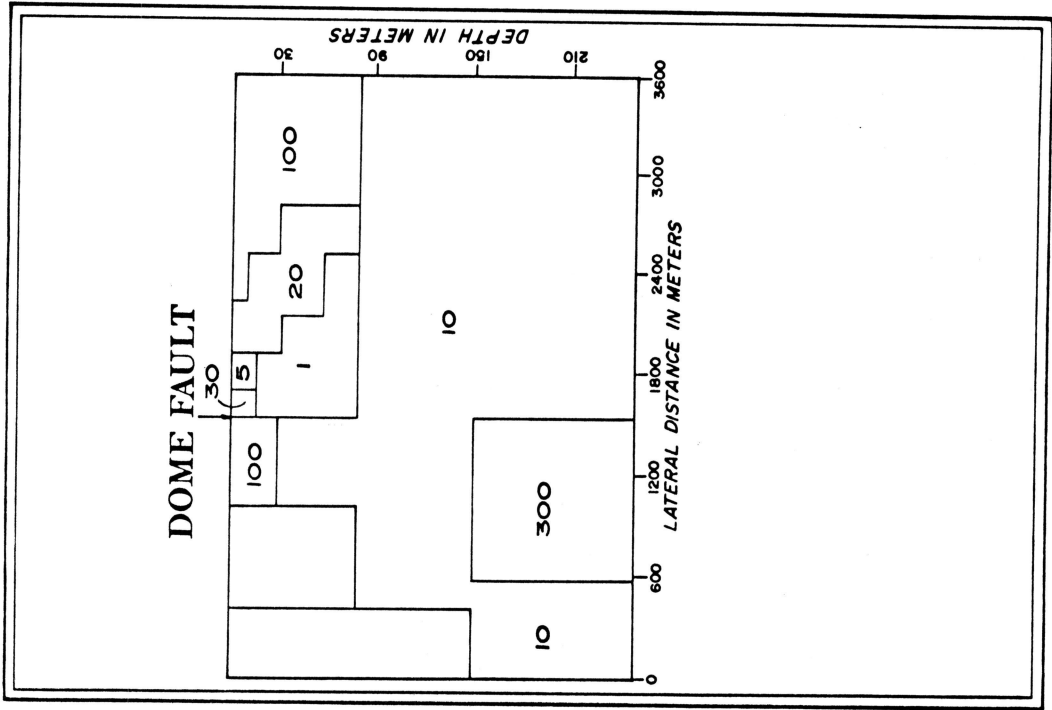


Figure 25

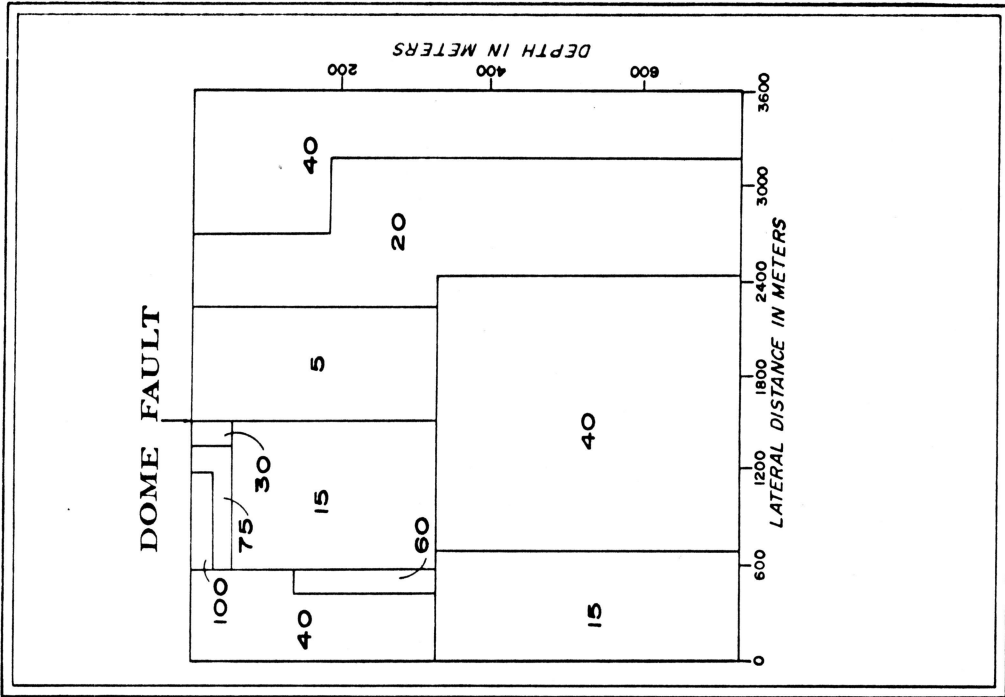


Figure 26

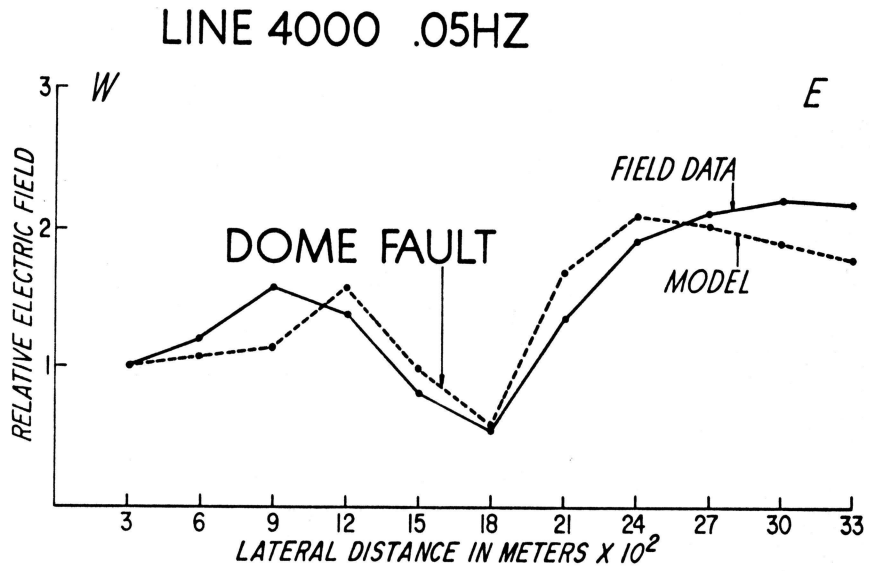


Figure 27

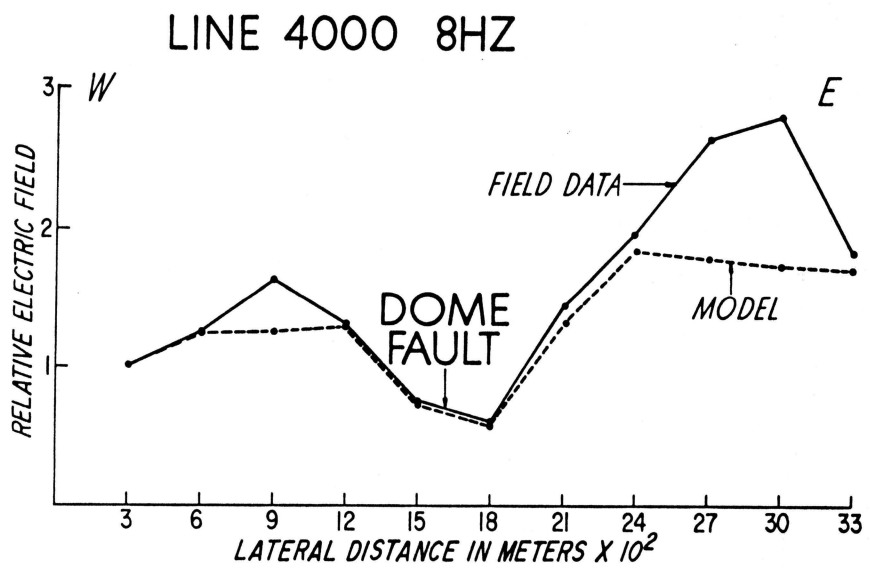


Figure 28

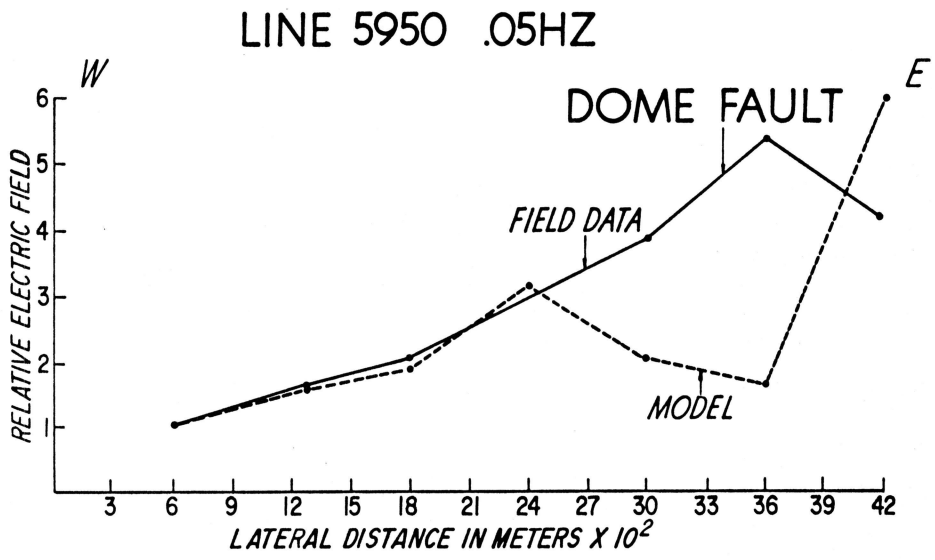


Figure 29

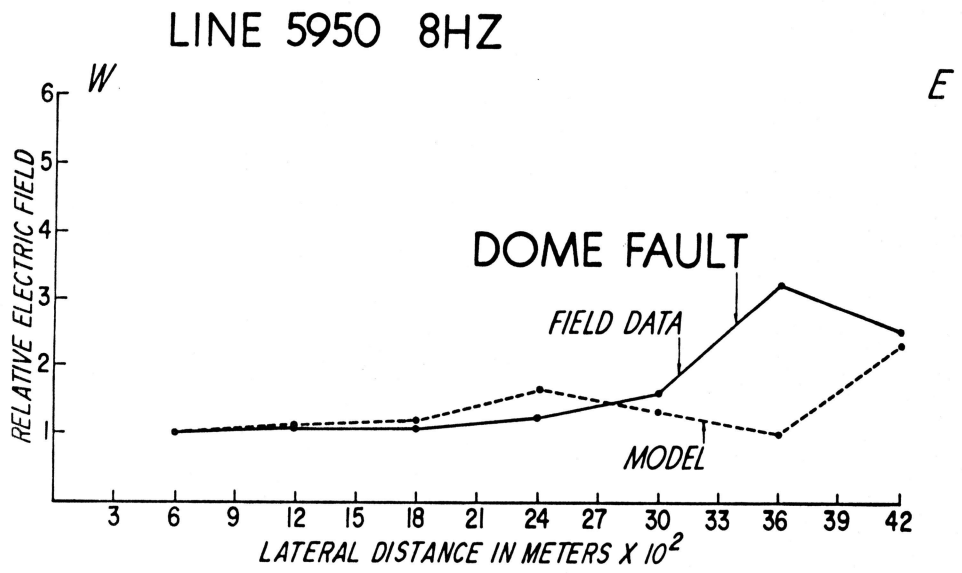


Figure 30

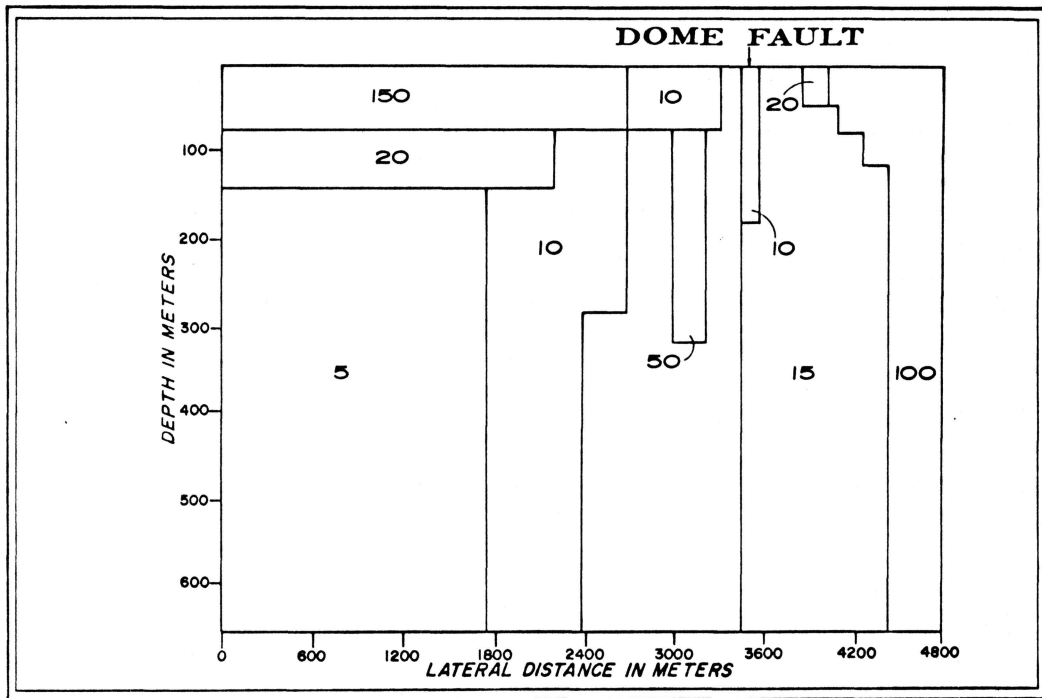


Figure 31

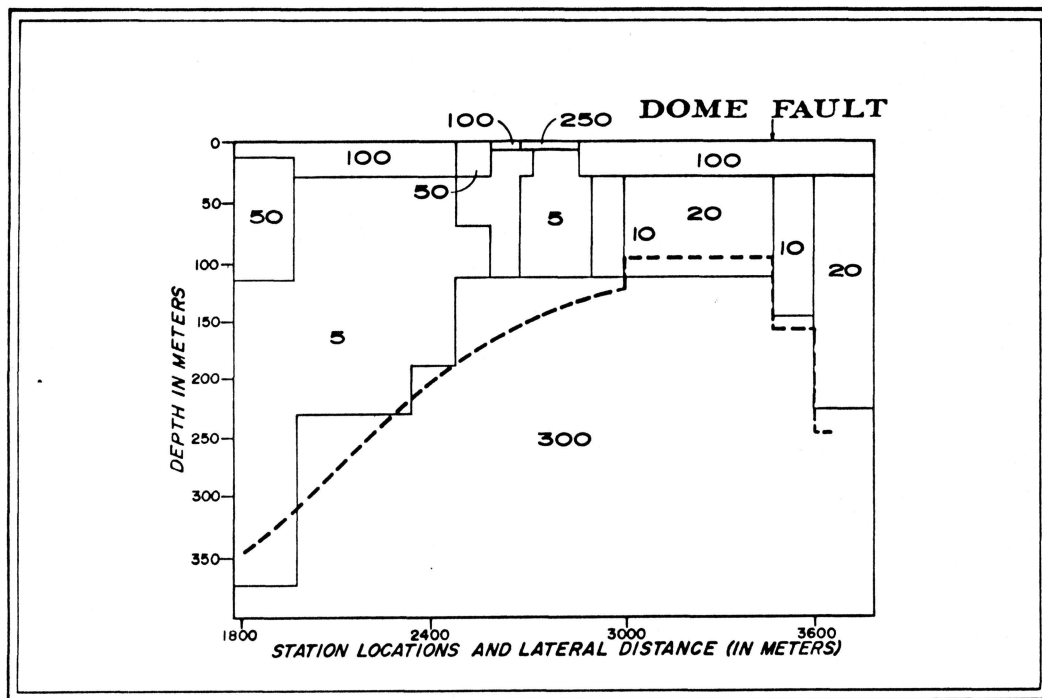


Figure 32

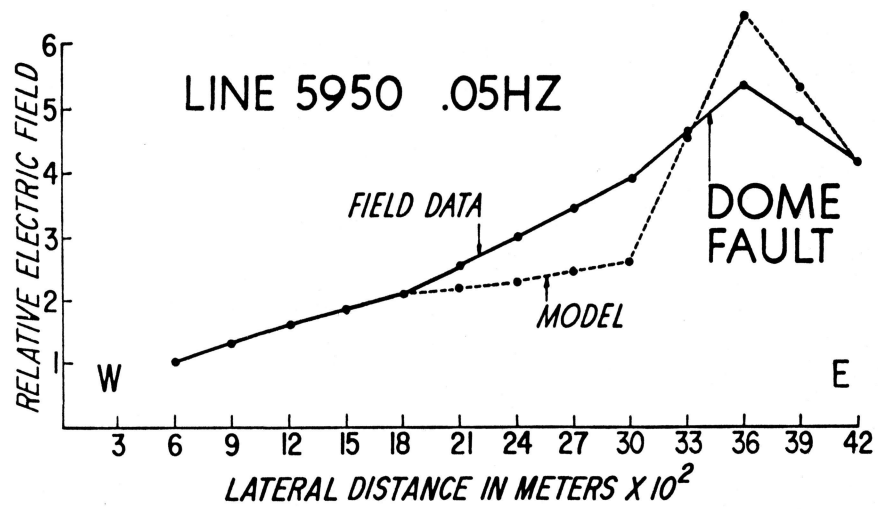


Figure 33

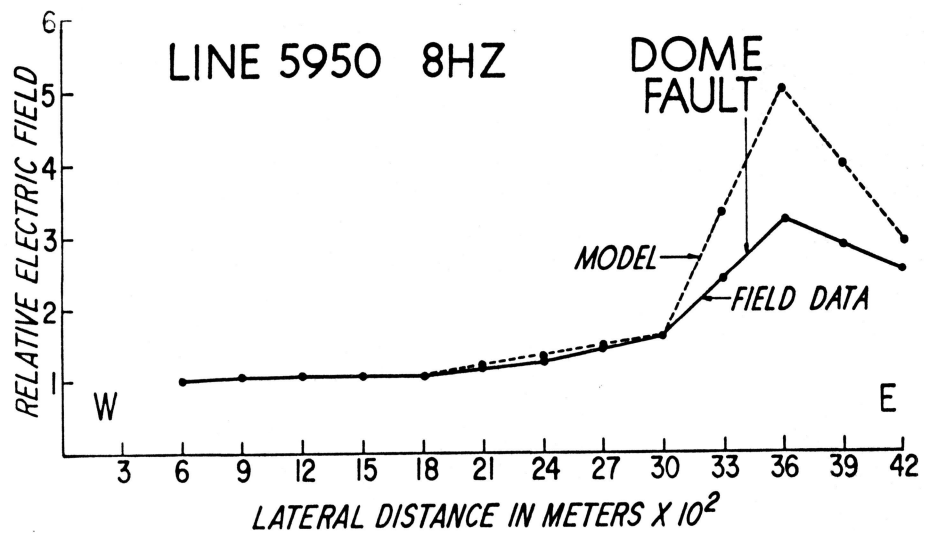


Figure 34

